GLUTAREDOXIN-2 CONTROLS MITOCHONDRIAL STRUCTURE AND ENERGETICS IN SKELETAL MUSCLE

Awa Liaghati

A thesis submitted in partial fulfillment of the requirements for the
Master's degree in biochemistry

Department of Biochemistry, Microbiology and Immunology
Faculty of Medicine
University of Ottawa

Abstract

Glutathione (GSH) plays a pivotal role in cellular redox poise, which is disordered in many metabolic diseases including type 2 diabetes. Glutaredoxin-2 (*Grx2*) is a glutathione transferase in mitochondria and the nucleus. We previously established that *Grx2* knockout ($Grx2^{-/-}$) mice have low GSH:GSSG and mitochondrial dysfunction in isolated mitochondria of muscle and heart. Moreover, low GSH:GSSG stimulates mitochondrial fusion in transformed cell lines. Our goal was to study the impact of $Grx2^{-/-}$ on the GSH ratio and on mitochondrial structure and function *in situ* and in intact primary muscle cells.

Compared to wild-type (WT), $Grx2^{-/-}$ myoblasts have a decreased GSH:GSSG, with a marked increase in mitochondrial length. Mitochondrial ultrastructure is profoundly abnormal in the $Grx2^{-/-}$ muscle compared to WT. Furthermore, mitochondrial content is significantly reduced in the $Grx2^{-/-}$ muscle. Mitochondrial energetic analyses in myofiber preparations confirm impaired CI activity and reveal impaired fatty acid oxidation capacity.

In summary, the absence of *Grx2* causes marked abnormalities in mitochondrial ultrastructure in skeletal muscle and in cellular GSH redox state and mitochondrial length.

Acknowledgements

First and foremost, I would like to extend my sincerest gratitude and deepest appreciation to my supervisor, Dr. Mary-Ellen Harper. Thank you for giving me the opportunity to be a student in your laboratory and for everything else that you have done for us over the last few years. I will never forget the sheer joy you gave me three summers ago when you accepted me into your laboratory. Your perpetual guidance, support, motivation and kindness are truly unparalleled and I could not have asked for a better supervisor. You can better your bottom dollar that Otis and I will be at your annual holiday gatherings!!

I would also like to thank my thesis advisory committee members, Dr. Morgan Fullerton and Dr. Katey Rayner, for their valuable suggestions, critical guidance and absolute kindness throughout my thesis. You two are wonderful professors with outstanding personalities!

A great big *thank you* goes to Dr. Chantal Pileggi, an exceptional post-doctoral fellow in the lab. My thesis would not have progressed so well without your detailed instructions, helpful assistance, witty sense of humor and incomparable motivation. We have had quite the accelerated friendship and I am beyond grateful to call you a dear friend of mine. Your personality is one that is irreplaceable and hard to find; in other words, you are amongst the few to truly understand me when I am being "extra." I am so honored to have met someone like you and shared my last laboratory experiences with you. Otis and I will be waiting for your visit to Montréal!

I also want to extend a special thank you to Dr. David Patten, a brilliant post-doctoral fellow in the lab. You have been so patient with me and my science math and an incredible help to my work. It has been an absolute pleasure teasing you in the laboratory, but above all, a pleasure to have created such a rapport with you. I can safely say you had a great influence on the person/scientist I am today. I wish you so much success in your future with your wonderful wife, Véronique and beautiful daughter, Elizabeth and unnamed second and third children. I will keep my eyes peeled for your publications in *Lancet, Science, Nature, Cell, PNAS etc.*, for you are a great scientist. You are a walking Encyclopedia and I *know* you will become one of the greatest professors, conducting ground-breaking research in the upcoming years.

To Abs, also known as Abi. You and I, we go way back; to the earlier days of "how to use a microscope." Your friendship, which I hold so dear to me, is one that does not come about often. You are genuine, honest, considerate, intelligent, and driven! Thank you for all the positivity and humor you have thrown at me over the last couple of years. You will accomplish some amazing goals in the next few years, starting from your Ph.D. defense to your Post-Doctorate Fellowship(s) to your tenure position as a professor. Don't forget me when you are a big-deal professor! You must visit me in Montréal for I will have no new friends. Thank you for being the person that you are and for choosing to be a friend of mine!

To my Saudi Princess, Rajaa. You have been the mother, the voice of reason, the motivator of the lab! You easily turned any and every one's frown upside down and it has been an

absolute pleasure getting to know you. You are a great scientist and your work ethic is extremely admirable. I will miss your optimism when I move, but I know you are just a phone call or text away. Your defense is right around the corner and you can count on me to be there, cheering you on as you have for me over the years. Thank you for everything, Rajaa, and best of luck with your thesis!

To Georges, my brother from another mother. I don't think you have ever hesitated in lending me a helping hand. For that, I sincerely thank you. I am so grateful and lucky to have had your knowledge, expertise, guidance and help throughout my thesis. You are a ray of sunshine, bursting with energy, joy and positivity! No wonder Dr. Harper always sent the new students to you; you always made it a priority to teach science the right way. I wish you so much success and happiness with Misha, as you two will begin a new life together. Be sure to keep me posted with your defense date and what the next chapter will be!

Jian, thank you for all the hard work you have done maintaining my mice colonies. You always made sure I was comfortable when it came to handling the mice and you were very helpful. Thank you so much!

Karan and Megan, I will place you both into the same paragraph as you are one entity now. It has been so fun getting to know you both as well as I do now. Karan, you are the little brother I never had. Megan, you are my other better half, with a bit more sass and a bit more class. I hope you both continue to crush your goals as medical students. Don't forget

me when you, Karan, become Canada's best ER doctor, or when you, Megan, become a national, leading pediatrician. You two made my toughest days a whole lot easier and when you two were not around, a dark cloud was hovering. Thank you for coming into my life, and please keep in touch Dr. Gandhi and Dr. MacFarlane.

I have saved the best for last: my mother, my father and my sister. *I dedicate this thesis and all my success to you three.*

My late-night calls, my temper tantrums, my stress and worries, my tears; you were all there for that. I do not know where I would be without my mother's care, my father's tough love and my sister's wise words. You three have carried me throughout my education, constantly telling me to never give up, to keep showing my fangs, to keep persevering, for one day it will all come together. And it did. Because of you.

If it's anyone who deserves a medal or a pat on the back, it is you three; I cannot even begin to imagine what it was like dealing with me as a stressful student monster, but I guess that's what families are for. You guys are the reason I keep moving forward, pushing for more success and achieving new goals.

If I was given the option to choose my family from birth, I would choose you three without any hesitation. You have given me the world and more. You have shaped me into the woman I am today. You guys make me want to be a better me every single day. I love you three so much and no amount of "thank yous" will ever show how grateful and lucky I am to have you as my support system.

By the way, in law school, the stress is only going to get worse, so keep those phones on standby!!

TABLE OF CONTENTS

ABBREVIATIONS

$\Delta\Psi_m$	Membrane potential
ΔpH	Proton gradient
βHAD	β-hydroxyl-CoA dehydrogenase
γ-GCS	γ-glutamylcysteine synthetase
ACS	Acyl-CoA synthase
ADP	Adenosine diphosphate
Akt	Protein kinase B
AMPK	5' AMP-activated protein kinase
ANOVA	Analysis of variance
ATP	Adenosine triphosphate
BNIP3	BCL2/adenovirus E1B 19 kDa protein-intereacting protein 3
BSA	Bovine serum albumin
CACT	Acylcarnitine translocase
CI	Complex I (ubiquinone NADH dehydrogenase)
CII	Complex II (succinate dehydrogenase)
CIII	Complex III (ubiqinol-cytochrome-c reductase)
CIV	Complex IV (cytochrome C oxidase)
CK	Creatine kinase
CPT	Carnitine palmitoyltransferase
Cyt C	Cytochrome C
DRP1	Dynamic-1-like protein
DTT	Dithiothreitol
ETC	Electron transport chain
$FADH^2$	Flavin adenine dinucleotide, reduced form
FAO	Fatty acid oxidation
FFA	Free fatty acids
GGT	γ-glutamyltranspeptidase
GLUT4	Glucose transporter 4
GPx	Glutathione peroxidase
GR	GSSG reductase
GRX	Glutaredoxin
GS	Glutathione synthetase
GS^-	Glutathione radical
GSH	Glutathione, reduced form
GSSG	Glutathione, oxidized form
GTPase	Guanosinetriphosphatase
IMF	Intermyofibrillar
LC3II	Light chain 3 phosphatidylethanolamine conjugate
LCFA	Long-chain fatty acids
MFF	Mitochondrial fission factor
MFN1/2	Mitofusin 1/2
MIM	Mitochondrial inner membrane

MOM	Mitochondrial outer membrane
MPTP	Mitochondrial permeability transition pore
mtDNA	Mitochondrial DNA
mTOR	Mechanistic target of rapamycin
NADH	Nicotinamide adenine dinucleotide, reduced form
NADPH	Nicotinamide adenine dinucleotide phosphate, reduced form
$NADP^+$	Nicotinamide adenine dinucleotide phosphate, oxidized form
nDNA	Nuclear DNA
NRF	Nuclear respiratory factor
OPA1	Optic atrophy 1
OXPHOS	Oxidative phosphorylation
PCr	Phosphocreatine
PDC	Pyruvate dehydrogenase complex
PGC1α	Peroxisome proliferator activated receptor coactivator 1 alpha
PPARD	Proliferator-activated receptor delta
PINK1	PTEN-induced putative kinase 1
PMF	Protonmotive force
ROS	Reactive oxygen species
SOD1	Superoxide dismutase (CuZnSOD)
SS	Subsarcolemmal
TCA	Tricarboxylic acid cycle
TFAM	Mitochondrial transcription Factor A
TG	Triglycerides
TIM	Translocase inner membrane
TMRE	Tetramethylrodamine ethyl ester
TOM	Translocase of the outer membrane
TRX	Thioredoxin
WB	Western blot

LIST OF FIGURES

CHAPTER I: INTRODUCTION

1.1. Overview of Skeletal Muscle

Skeletal muscle is an intricately organized organ that functions to contract, generate force and produce movement. Skeletal muscle accounts for 40% of total body weight in lean adults[1], making it the most abundant tissue in the body. Skeletal muscle displays a high level of plasticity, adjusting its size and molecular make up in accordance to a variety of external stimuli, including mechanical load, nutritional status, different growth factors and hormone fluctuations in the body. Skeletal muscle is widely known as a major site of metabolic activity, acting as an important sink for glucose uptake and fatty acid utilization, accounting for ~70-80% of whole body insulin-stimulated glucose uptake[2]. The breakdown of glucose includes the glycolytic pathway, the tricarboxylic acid (TCA) cycle and the electron transport chain (ETC). The final product of these oxidative pathways is adenosine triphosphate (ATP), the cellular energy 'currency.' These pathways, excluding glycolysis, are located in the mitochondrion, which are believed to have emerged through an endosymbiotic relationship with bacteria[3]. Mitochondria are indispensable organelles, responsible for transducing energy and maintaining cellular metabolic homeostasis. In addition to energy transduction, mitochondria are involved in cellular differentiation, apoptosis, redox regulation, mitochondrial DNA maintenance, reactive oxygen species (ROS) production and more[4,5]. Therefore, it is important to understand the structure and the function of mitochondria to improve metabolism in skeletal muscle.

1.1.1 Metabolic Activity in Skeletal Muscle

Skeletal muscle contains 50-75% of total body proteins[1]. Skeletal muscle is a highly malleable tissue capable of adapting to several different metabolic and morphological challenges. Beyond its role in regulating metabolism through glucose disposal, skeletal muscle serves as a reservoir for amino acids and carbohydrate, and contributes to heat production to maintain core temperature. Because skeletal muscle can store amino acids, *de novo* protein synthesis occurs, which is a vital process for other tissues such as skin, brain and heart[6]. Furthermore, the release of amino acids from skeletal muscle contribute to the maintenance of blood glucose levels through liver gluconeogenesis[1].

Since the metabolic rate of skeletal muscle can increase close to one hundred times between rest and work, it is regarded as one of the ideal tissues for studying metabolism[7]. The metabolic activity of skeletal muscle depends on several factors, such as fiber type composition, nutritional status, hormone balance and physical activity. Regulation of circulating levels of glucose is a fundamental characteristic of metabolic homeostasis and insulin is the main hormone involved in regulating glucose uptake.

Tissues that exhibit insulin-mediated glucose uptake (*i.e.* skeletal muscle, cardiac muscle and fat) contain two isoforms of the glucose transporter proteins, GLUT1 and GLUT4[8]. GLUT1 is targeted at the plasma membrane and is believed to mediate glucose uptake in the basal state[9,10]. Glucose uptake can occur in two different states: the contraction state or the insulin-stimulated state. GLUT4 is one

of 13 facilitative glucose transport proteins and is highly expressed in skeletal muscle[11]. In contracting muscle, glucose uptake occurs via facilitated diffusion, which is contingent on the translocation of GLUT4 transporter from intracellular sites to the sarcolemmal membrane[11,12]. When glucose, and subsequently insulin levels increase in the blood, insulin binds to its receptor on the sarcolemmal membrane and recruits GLUT4 to the membrane.

Once glucose has been transported into the muscle cell, it can be stored as glycogen or metabolized through glycolysis. The product of glycolysis, pyruvate, can be further oxidized in mitochondria. Through the oxidative processes, the final product, ATP, is generated, which is the main energy source used during muscle contraction. Intracellular ATP stores in skeletal muscle are exceedingly small, ~5-6 mM, and when the muscle is fully activated, ATP stores are depleted within 2 seconds[13]. Thus, ATP-generating pathways are activated during bouts of contraction to avoid total ATP depletion. These pathways can be categorized into anaerobic and aerobic pathways.

1.1.1.1 Anaerobic Metabolism

Anaerobic metabolism occurs in the absence of oxygen and the two main processes that regenerate ATP are the degradation of phosphocreatine (PCr) and the breakdown of muscle glycogen to produce lactate. The degradation of PCr is achieved through the enzyme creatine kinase (CK), which catalyzes the following reaction: PCr + ADP (adenosine diphosphate) ⇔ Cr + ATP. When

ATP consumption is high, the reaction is driven forward, thereby decreasing PCr concentrations and increasing creatine concentrations, while ATP concentrations remain nearly constant.

The breakdown of glycogen occurs via glycogen phosphorylase that can either exist in its phosphorylated, active form or non-phosphorylated, less active form. The phosphorylation of glycogen phosphorylase is catalyzed by phosphorylase kinase and its de-phosphorylation by protein phosphatase[14]. During glycogenolysis, glucose is released from glycogen by glycogen phosphorylase and enters glycolysis to be converted to pyruvate. When ATP consumption is high in skeletal muscle (*i.e.* during high-intensity training), lactate and hydrogen ions begin to accumulate. However, increased lactate production poses a disadvantage because the ATP yield is much less per glucosyl unit compared to aerobic metabolism (*i.e.* 2 ATP produced during anaerobic respiration compared to a maximum of 38 ATP during aerobic respiration)[15].

1.1.1.2 Aerobic Metabolism

Aerobic metabolism occurs under the presence of oxygen and is more efficient at producing ATP than glycolysis[16,17]. Skeletal muscle exhibits metabolic flexibility in that it can use either carbohydrates or lipids as energy sources, and the oxidative

metabolism of these substrates are the prevailing ATP-producing pathways. The oxidation of lipids in muscle occurs predominantly during periods of fasting, whereas glucose is utilized during postprandial periods. Carbohydrate fuel sources, either from the intestine or from glycogen stores in liver or muscle, provide glucose, which is then transported into the cell for oxidation. In addition to storing amino acids, skeletal muscle can store small amounts of fat in the form of triglycerides (TG). From these TG stores, free fatty acids (FFA) undergo lipolysis and become the substrate for lipid metabolism. Furthermore, at rest, skeletal muscle predominantly uses FFA as the fuel source[18].

The first step in aerobic metabolism of glucose is glycolysis, which occurs in the cytoplasm. After glucose is taken up by the muscle cells via GLUT4, it is phosphorylated, transforming glucose to glucose 6-phosphate. Nine subsequent steps are achieved to reach a final product of pyruvate. Pyruvate is transported into the mitochondrion through the pyruvate translocase antiporter and can enter the TCA cycle, which also takes place in the mitochondrial matrix. Pyruvate will undergo oxidative decarboxylation by the pyruvate dehydrogenase complex (PDC), which is the link between glycolysis and the TCA cycle[19]. The TCA cycle, also referred to as the Krebs cycle or the citric acid cycle, is the pathway in which

glycolysis and β-oxidation products converge. When the acetyl-CoA molecule enters the TCA cycle, it will undergo eight enzymatic reactions to generate the electron carriers NADH and $FADH_2$, that will donate electrons to the complexes of the ETC[20]. Isocitrate dehydrogenase is the enzyme that catalyzes the conversion of isocitrate to α-ketoglutarate and is one of the rate-controlling steps in the TCA cycle. This enzyme is stimulated by ADP and inhibited by ATP[21], demonstrating the tight regulation in the production of ATP. Moreover, the rate-controlling enzymes of the TCA cycle are major targets of the mitochondrial calcium import pathway as they are upregulated by calcium-dependent processes[22]. In other words, intra-mitochondrial calcium activates the rate-controlling enzymes of the TCA cycle, thereby increasing oxidative phosphorylation (OXPHOS) and ATP synthesis[23].

1.2. Skeletal Muscle Oxidative Capacity

The oxidative capacity of skeletal muscle is defined as the ability of muscle to utilize oxygen to produce ATP[24]. Reduced oxidative capacity in skeletal muscle has been associated with decreases in mitochondrial density[25]. To maintain optimal mitochondrial function, as well as ensuring the function of skeletal muscle, constant renewal of mitochondria is required[26]. Mitochondrial biogenesis (or mitochondriogenesis) is the process by which mitochondria are newly synthesized. Mitochondriogenesis in muscle cells is initiated by muscle contraction[27] and is

stimulated by the proliferator-activated receptor delta (PPARD)-peroxisome proliferator-activated receptor γ coactivator 1α (PGC1-α)-nuclear respiratory factor (NRF)-mitochondrial transcription Factor A (TFAM) pathway[28]. Briefly, PPARD induces the promotion of PGC1-α[29], which is the first stimulator of mitochondriogenesis. This is followed by NRF1 and 2, which stimulate the synthesis of TFAM, that will activate the duplication of mitochondrial DNA molecules[30]. Furthermore, it has been demonstrated that under conditions that lead to ATP depletion (*e.g.* muscle contraction), mitochondrial content increases[27]. This is because the increased rate of ATP turnover (*i.e.* ATP synthesis and degradation) is sufficient to provoke mitochondriogenesis[27].

1.2.1 Mitochondrial Structure

Mitochondria account for ~20% of the mass of eukaryotic cells[31], but this is highly variable and dependent on cell types. They are 0.1-1.0 μm in diameter and 1-2 μm in length[32,33], and consist of an outer membrane, inner membrane with invaginations known as cristae, intermembrane space and a matrix. The mitochondrial outer membrane (MOM) separates the mitochondria from the cytosol and allows the passage of metabolites. The main transport molecule on the MOM is porin, which allows the movement of molecules with a molecular weight of 5000 Daltons or less[34,35]. Mitochondria contain between 1000-1500 different proteins, with only a few encoded by their 16 kb circular DNA[31,36,37]. Mitochondrial DNA (mtDNA) is double stranded and contains 37 genes for 13 polypeptides, all of which are subunits of the complexes of the ETC[36]. The remaining mitochondrial proteins,

approximately 98%[31], are encoded by the nuclear genome and synthesized on cytosolic ribosomes. Therefore, those proteins must be imported into mitochondria and the translocase of the outer membrane (TOM) provides the entry gate[38]. The mitochondrial inner membrane (MIM) is impermeable to ions since its lipid bilayer is composed of cardiolipin, a "double" phospholipid that has four fatty acids[32]. However, small proteins are shuttled into the matrix via the translocase inner membrane (TIM)[39]. The two driving forces for protein transport across the inner membrane are the membrane potential across that membrane and the hydrolysis of ATP in the matrix[31]. The inward projections of the MIM are referred to as cristae, which are studded with proteins and increase the surface area for the OXPHOS system[40,41]. The two aqueous compartments of the mitochondrion are the intermembrane space and the matrix. The intermembrane space is the space between the MOM and the MIM[33]. Cytochrome *c*, located on the outer surface of the MIM, which shuttles electrons between complex III and complex IV of the ETC, is the most abundant protein in the intermembrane space[42]. Since the matrix contains approximately 67% of total mitochondrial proteins, many of the metabolic processes occur within this area[32].

1.2.2 Mitochondrial Function

In skeletal muscle, mitochondria can be found in two distinct regions: subsarcolemmal (SS) and intermyofibrillar (IMF). The SS mitochondria account for approximately 10-15% of the mitochondrial fraction[43]. Mitochondria are widely recognized as the "powerhouse" of the cell. Mitochondrial energy transduction is

driven by ADP import from the cytosol. It is then converted to ATP by OXPHOS through the ETC[44]. Pyruvate, from glycolysis, is transported into the mitochondrial matrix where it is decarboxylated to acetyl CoA by the PDC. This acetyl CoA, and the acetyl CoA from FA oxidation, enter the TCA cycle and undergoes a series of reactions that release electrons (also called reducing equivalents) to the electron carriers nicotinamide adenine dinucleotide (NADH) and flavin adenine dinucleotide ($FADH_2$). NADH and $FADH_2$ donate the electrons to the ETC that are passed along the complexes of the ETC. Mitochondria are efficient at producing enough ATP to sustain cellular functions; mitochondria produce 90% of a cell's ATP and ~90% of the oxygen consumed is utilized in the ETC for OXPHOS[45]. However, mitochondrial coupling of ATP synthesis and substrate oxidation is not as efficient; protons can travel back to the matrix independent of ATP synthase[46]. This process is known as "proton leak." Proton leak occurs under basal conditions and can account up to 50% of skeletal muscle respiration in rats[47].

1.2.1.1 β-oxidation and the Tricarboxylic Acid Cycle

OXPHOS is driven by reducing equivalents that have been generated through the oxidation of cellular fuels such as fatty acids. Fatty acid transporters located on the plasma membrane facilitate the uptake of FFAs into the muscle cell. These transporters include the fatty acid translocase (FAT/CD36)[48,49], the fatty acid transport protein (FATP-1)[50] and the plasma membrane fatty acid binding protein (FABPpm)[51]. For entry into the mitochondria, where fatty acid oxidation occurs, short and medium chain

fatty acids enter through passive diffusion. However, long-chain fatty acids (LCFA) rely on the carnitine palmitoyltransferase (CPT) system. This system consists of three proteins: CPT1, acylcarnitine translocase (CACT) and CPT2[52]. LCFAs are esterified by the enzyme acyl-CoA synthase (ACS), forming LCFA-CoA, which is the substrate for mitochondrial CPT1[53]. CPT1 is a rate-controlling step in FAO because it is tightly regulated by malonyl-CoA, a product produced by glucose metabolism[53]. CPT1 regulates the movement of fatty acid acyl groups into the intermembrane space through the exchange of coenzyme A for carnitine. The CACT, located on the mitochondrial inner membrane (MIM), allows the fatty acyl carnitine to enter the mitochondrial matrix and is converted back to acyl-CoA by CPT2[53,54]. Once inside the mitochondrial matrix, β-oxidation occurs in a four-step process by the following enzymes: fatty acyl-CoA dehydrogenase, β-hydroxyl-CoA dehydrogenase (βHAD), hydroxyacyl-CoA dehydrogenase and acetyl-CoA transferase. By cleaving two carbons every cycle, the products generated by β-oxidation are acetyl-CoA molecules, which will enter the TCA cycle.

1.2.1.2 Oxidative Phosphorylation and the Electron Transport Chain

The OXPHOS system is located on the MIM and consists of four enzyme complexes and the ATP synthase[55]. Electrons are transferred along complexes I-IV (Fig. 1.1) due to Gibbs free energy, which is stored across

the MIM and is defined as the energy available to do work[56]. These complexes will undergo conformational changes to pump protons from the mitochondrial matrix to the intermembrane space. Complex I (NADH-Q oxidoreductase) is the largest of the respiratory complexes, consisting of 45 core subunits[57]. Complex I accepts electrons from NADH, oxidizing it to NAD^+ and pumps protons into the intermembrane space while reducing ubiquinone[58]. Succinate dehydrogenase, an enzyme involved in the TCA cycle that generates $FADH_2$ from the oxidation of succinate to fumarate, is part of complex II (succinate-Q reductase), which consists of four protein subunits[59]. $FADH_2$ remains in the complex and the electrons are transferred to coenzyme Q for entry into the ETC[59]. The electrons from complex I are carried to complex III by ubiquinone, which diffuses readily within the MIM. Complex III (Q-cytochrome *c* oxidoreductase) catalyzes the transfer of electrons from ubiquinol to cytochrome *c* and pumps protons into the intermembrane space. Electrons delivered to complex III are carried to complex IV (cytochrome *c* oxidase) by cytochrome *c*. Complex IV reduces O_2 to H_2O, while simultaneously pumping protons into the intermembrane space. The proton pumping function of complexes I, III and IV generates a proton gradient that is dissipated through complex V (ATP synthase), driving the phosphorylation of ADP to ATP[60]. ATP synthase is composed of two protein entities: the F_1, which is located in the mitochondrial matrix, and the F_o, which is bound to the MIM. Through the F_o portion of ATP synthase, protons cross the MIM from the intermembrane space to the

matrix[61]. The proton gradient (ΔpH) contributes to the protonmotive force (PMF) across the MIM. The other component of PMF is the membrane potential ($\Delta\Psi_m$)[62]. The flow of protons down this electrochemical gradient, via ATP synthase drives ATP synthesis[62], thus marking it as an essential feature of the mitochondrion[63]. The PMF is vital for other mitochondrial functions, such as protein import[64] and can be used as a trigger to cause changes in response to mitochondrial dysfunction[5]. Furthermore, when the $\Delta\Psi_m$ is high, the mitochondrial permeability transition pore (MPTP) is inhibited[65]. The MPTP is a non-specific channel located in the MIM. Under certain conditions, including calcium overload[66], increased oxidative stress[67], adenine nucleotide depletion[68] and elevated phosphate levels[69], the MPTP opens which allows the free passage of solutes <1.5 kDa into the mitochondria[65].

Within the ETC, complexes I and III, have been shown to leak electrons during cellular stress, resulting in ROS formation[70,71]. Since contracting muscles are known to produce ROS, it is not surprising that skeletal muscle mitochondria contain several antioxidant defense systems, including the glutathione (GSH) system. Arguably, GSH is one of the most important antioxidants in muscle fibers, both enzymatically, as GSH peroxidases (GPx), and non-enzymatically. In recent years, there has been major progression in understanding the complexity behind GSH and its function in several different tissue types. However, very little is known about GSH

redox perturbations and how it affects mitochondrial structure and function in muscle cells and myofibers. Furthermore, the mechanism in which GSH redox status is controlled by the mitochondrial/nuclear oxidoreductase glutaredoxin-2 (*Grx2*) remains elusive. Thus, understanding the molecular mechanisms that elucidate GSH ratio imbalances in muscle mitochondrial health can enhance the understanding of the interplay between redox environment and metabolic activity in skeletal muscle.

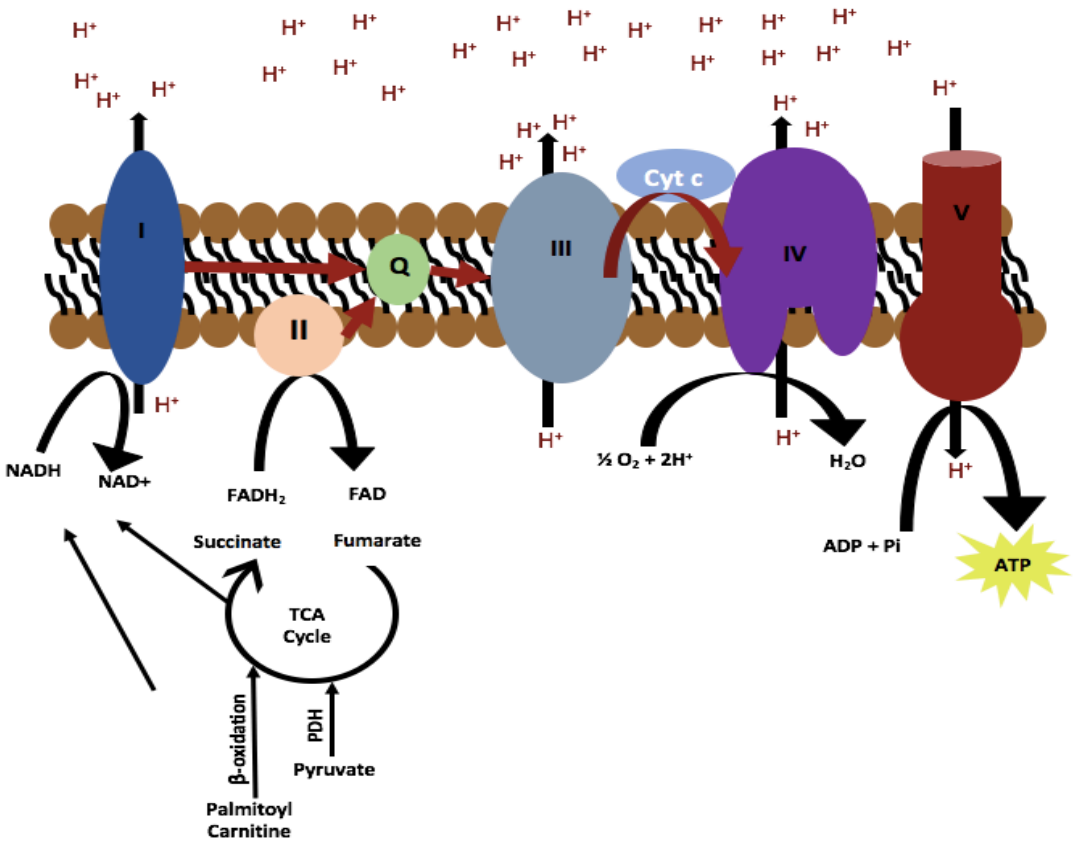

Figure 1.1. Electron flow through the complexes of the electron transport chain. Glucose and FFA metabolism occurs via glycolysis and β-oxidation, respectively, which feed into the TCA cycle. TCA cycle generates NADH + H^+ and $FADH_2$, which donate electrons into the complexes I and II of the ETC, respectively. Electrons are carried to complex III and complex IV, where O_2 is reduced to H_2O. This produces the proton gradient that drives ATP synthesis at complex V.

1.2.1.3 Mitochondrial fusion and fission

Recent research has firmly established that mitochondria are highly dynamic organelles that migrate throughout the cell, and are continuously undergoing processes of fusion and fission[72]. Mitochondrial dynamics, which collectively refers to mitochondrial fusion and fission processes, plays a critical role in maintaining functional mitochondria and have been associated with pivotal cellular processes, such as mitophagy, mitochondrial DNA maintenance, apoptosis, quality control and intracellular signaling[5,73,74,75]. Mitochondrial fusion is thought to occur to allow mitochondria to exchange content, which mitigates stress levels and prevents the accumulation of mtDNA mutations and oxidized proteins[76]. Fusion also contributes to cross-complementation between two damaged mitochondria, thus maximizing oxidative respiratory capacity in response to stress stimuli[77]. In contrast, fission occurs to produce new mitochondria and initiates the removal of damaged components[77]. Fission is also important in promoting mitochondrial turnover, adjusting for mitochondrial volume under different metabolic conditions[78]. Mitochondrial fusion is mediated by the guanosinetriphosphatase (GTPase) dynamin family of proteins. The proteins involved in mitochondrial fusion include mitofusin 1 and mitofusin 2 (Mfn1 and Mfn2), located on the MOM, and optic atrophy 1 (OPA1), located on the MIM (Fig. 1.2). Mfn1 and Mfn2 initiate the first steps of fusion by fusing the mitochondrial outer membranes of adjacent mitochondria[79]. Mfn2 is a key protein involved in metabolism as it

upregulates glucose oxidation through the increased expression of several subunits in complexes I, IV and V of the ETC[80,81]. The final step in fusion is the tethering of the MIM by OPA1, which also plays an important role in cristae maintenance[82,83]. In contrast, the proteins that promote fission include the dynamin-related protein 1 (DRP1), fission protein 1 (Fis1) and mitochondrial fission factor (Mff) (Fig. 1.2). DRP1 is a cytosolic protein that must be recruited to the MOM for fission to be initiated. Mff acts as a binding site for DRP1, thereby recruiting it to the outer membrane[84,85]. Once DRP1 is recruited, it constricts the MOM and forms spirals around the mitochondria, which leads to the division of the organelle. If cellular stress increases within the cell and/or a loss in mitochondrial membrane potential occurs, mitochondria begin to segregate for degradation by mitophagy[86]. It has been repeatedly demonstrated that when mitochondrial fission is reduced, mitophagy is attenuated, suggesting that fission might be a requisite for mitophagy to occur[86,87,88].

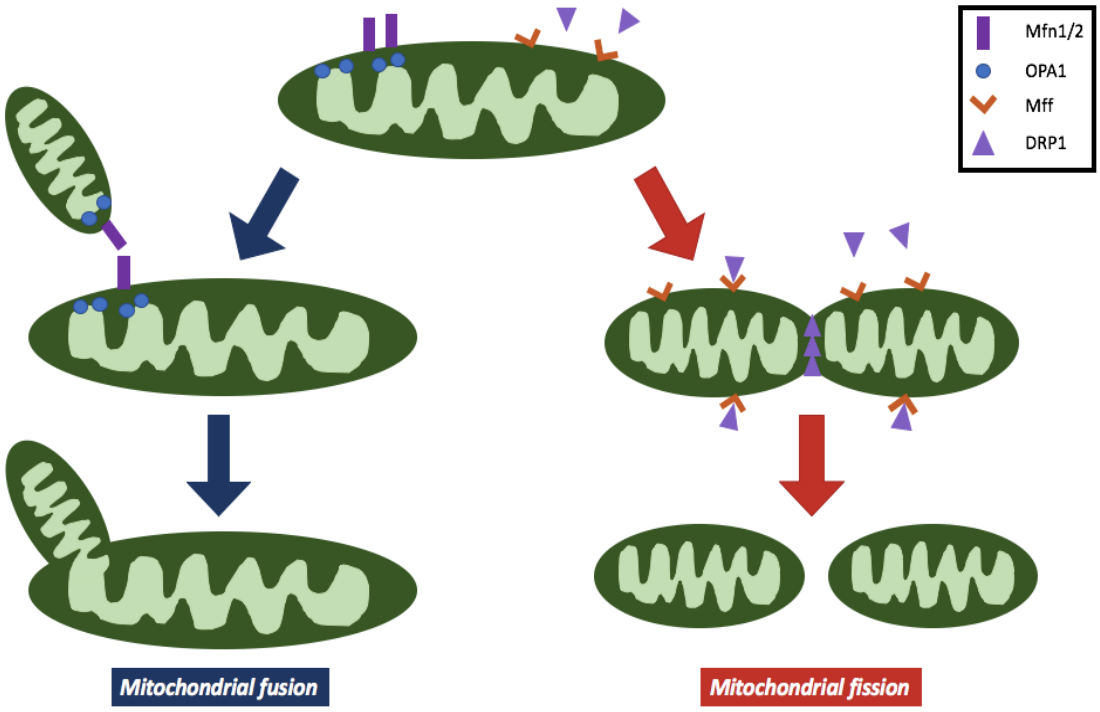

Figure 1.2. Mitochondrial fusion and fission events mediated by GTPases. Mitochondrial fusion includes Mfn 1 and 2, which fuse the mitochondrial outer membranes, and OPA1, which fuses the mitochondrial inner membranes of two separate mitochondria. In mitochondrial fission, Mff, located on the mitochondrial outer membrane, recruits DRP1 from the cytosol and acts as a binding site for

1.2.1.4 Mitophagy

Autophagy is an evolutionary conserved cellular process essential for maintaining the health of an organism. It is responsible for the degradation of components via the lysosomal pathway[89]. Mitophagy is defined as the selective removal of damaged or dysfunctional mitochondria by autophagosomes through the autophagy pathway[90] and is essential in sustaining mitochondrial homeostasis following any metabolic changes[78]. The serine/threonine kinase PTEN-induced putative kinase protein 1 (PINK1), found in the intermembrane space, is an important regulator of mitophagy[91] and is found at very low levels with intact membrane

potential[91]. Parkin, an E3 ubiquitin ligase, is found in the cytosol under basal conditions. However, upon loss of mitochondrial $\Delta\Psi_m$[92,93], normal degradation of PINK1 is blocked and begins to accumulate on the MOM[94]. The accumulation of PINK1 induces the translocation of Parkin to the mitochondria and mitophagy is initiated[95]. Parkin then ubiquitinates mitochondrial proteins, which serves as a signal for the initiation of mitophagy[96]. To date, there are four mitochondrial targets for Parkin ubiquitination: VDAC1[96], Mfn1 and Mfn2[97,98] and MIRO[99]. The adaptor protein, p62/SQSTM1 (hereafter referred to as p62), binds to both the ubiquitinated mitochondrial proteins[100] and the microtubule associated protein 1 light chain 3 (LC3) on the phagophore[101]. LC3, which is an autophagosomal marker, can only associate with the phagaphore once it has begun to form[102]. The binding of p62 to the ubiquitinated proteins anchors the mitochondrion to the LC3[91]. LC3II, which is membrane bound and conjugated to phosphatidylethanolamine, initiates the encapsulation of mitochondria into autophagosomes[103]. The autophagosome will then fuse with lysosomes for degradation by lysosomal enzymes[89]. Furthermore, the BH3-only protein, Bnip3, is an autophagy receptor that signals degradation of mitochondria (mitophagy)[104]. In healthy cells, mitophagy is tightly regulated and coupled with mitochondrial biogenesis[91,105]. Excess mitophagy can promote cell death[106]; therefore, in response to increased mitophagy events, mitochondria possess a reserve capacity that helps maintain energy production[107]. In contrast, insufficient mitophagy can

result in the accumulation of mtDNA mutations, thereby leading to oxidative damage[108]. Therefore, the process of mitophagy is crucial in maintaining proper mitochondrial function and in preventing the activation of cellular apoptosis[103].

1.3. Glutathione Redox

GSH is the most abundant non-protein antioxidant within mitochondria[109] and mammalian cells[110]. GSH is ubiquitous in eukaryotes and plays an important role in cellular functions and metabolism[111]. There are three major GSH reservoirs: cytosol, mitochondria and endoplasmic reticulum[112]. GSH levels vary between tissue types and it appears to be associated to the oxidative capacity of the tissue[113]. The majority of total body GSH is found in skeletal muscle[114], with concentrations ranging between 0.5 to 3 mM[115]. GSH exists predominantly in its reduced form (GSH)[116,117], but upon the neutralization of reactive oxygen species, GSH becomes oxidized (GSSG)[118]. GSSG is regarded as an indicator of cellular stress[119]. Of the three most important redox couples, the GSH redox pair (GSH:GSSG) is approximately 500- to 1000-fold higher in concentration than the NADPH and TRX systems[120]. Therefore, any changes in the GSH:GSSG is a direct reflection of the intracellular redox status[121,122]. In resting and healthy cells, the GSH:GSSG ratio is greater than 100:1[116,121], however, in cases of oxidative stress, this ratio can decrease to 10:1 or even 1:1[123]. Superoxide and/or hydroxyl radicals oxidize GSH at high rates[124]. However, due to its high intracellular concentration, GSH acts as a powerful reducing agent, thus preventing the accumulation of oxidized compounds.

The apparent fundamental function of GSH is to provide cells with a reducing environment and to neutralize free radicals[114]. Since skeletal muscle has low levels of catalase and superoxide dismutase enzymes, it is believed that GSH is the major compound involved in detoxifying ROS[114]. Recent literature estimates that mitochondria contain similar GSH concentrations to those in the cytosol (between 1 to 14 mM)[125]. The redox status of the mitochondria is not dependent on the cytosolic redox status and is strictly regulated[109]. The rapid turnover rate of GSH is a result of GSSG reductase (GR) in the mitochondria, which has a high affinity for GSSG[124] and thus, reduces GSSG back to GSH. However, since mitochondria are devoid of the machinery to synthesize GSH, they rely on GSH import from the cytosol[126]. The mitochondrial GSH pool is critical in preventing and repairing oxidative damage that is normally generated under physiological aerobic metabolism[71,127]. The depletion of GSH in skeletal muscle has been shown to cause mitochondrial degeneration[114], which demonstrates the importance of maintaining a sufficient GSH pool to support mitochondrial functions. Furthermore, other studies in rats show that depletion of cellular GSH leads to mitochondrial damage and apoptosis[128,129].

1.3.1 Glutathione Synthesis Pathway

GSH (γ-L-glutamyl-L-cysteinylglycine) is a tripeptide molecule, composed of cysteine, glycine and glutamate. Many of the functions carried out by GSH are linked to redox reactions of the cysteine sulfur group[124]. While GSH is endogenously produced in the cytosol in virtually all cell types[130], it can be

transported into cells from the circulation, and the main source of GSH for release into the blood is the liver[130,131]. GSH can be synthesized in three ways: *de novo* synthesis via a two-step, ATP-dependent process (Fig. 1.3), the regeneration of GSH from GSSG by GR and the recycling of cysteine from γ-glutamyltranspeptidase (GGT). The first reaction from *de novo* synthesis involves γ-glutamylcysteine synthetase (γ-GCS), which is the rate-limiting step[130], and the second reaction involves GSH synthetase (GS). In the first reaction, γ-GCS forms an unusual peptide bond between the γ-carboxyl group of glutamate and cysteine using the energy released by ATP hydrolysis[112]. In the second reaction, the addition of glycine to γ-glutamylcysteine, to form GSH, is catalyzed by GS using the energy from ATP hydrolysis[131]. Once γ-glutamylcysteine is synthesized, it is rapidly converted to GSH, demonstrating the non-regulatory role of GS[132]. In models of high oxidative stress where GSH is depleted, *de novo* synthesis is upregulated by increasing the availability of cysteine through the breakdown of GSSG[121]. GR contributes to the regeneration of GSH by maintaining the total GSH pool in a reduced state via the cyclic reduction of GSSG[117]. The structure of GSH is unique because the peptide bond linking glutamate to cysteine is through the γ-carboxyl group of glutamate instead of the α-carboxyl group[112]. The only enzyme that can initiate catabolism of GSH via the peptide bond is GGT[112], which is only present on certain cell types[133]. Therefore, GSH becomes resistant to intracellular degradation and can only be metabolized by cells that express GGT. Once GSH is catabolized, its amino acids can be taken up by cells to regenerate GSH. The rate of GSH synthesis is regulated by γ-GCS levels[134], the availability of L-cysteine

(often limiting due to liver concentrations of 15-500 μM)[130,135] and feedback inhibition of γ-GCS by GSH[136]. L-glutamate and L-cystine share an antiporter, which exchanges extracellular L-cystine with intracellular L-glutamate[137]. If extracellular levels of L-glutamate are high, then the uptake of L-cystine is competitively inhibited, thereby inhibiting the uptake of L-cystine and thus its availability for GSH synthesis[138]. The levels of GSH, both intracellularly and extracellularly, depend on the balance between production, degradation and transportation.

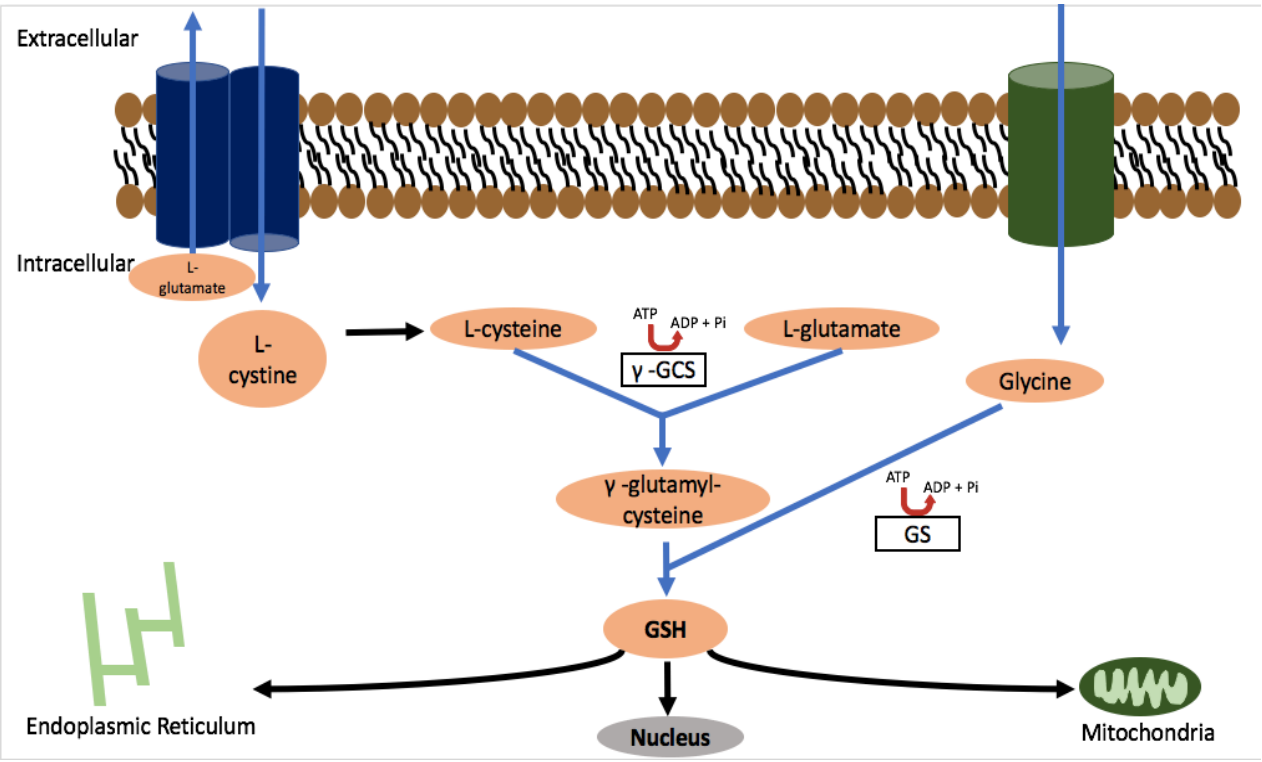

Figure 1.3. Glutathione synthesis pathway. GSH is synthesized exclusively in the cytosol, in a two-step, ATP-dependent process. GSH can be found in the nucleus, mitochondrion and endoplasmic reticulum.

1.3.2 Antioxidant Function of Glutathione

GSH is an abundant cellular antioxidant[139] with a redox potential between -260 to -200 mV in the cytosol and -330 to -300 mV in the mitochondria[140]. These characteristics make GSH an excellent compound in detoxifying ROS, drugs and xenobiotics, thereby attenuating oxidative stress. GSH is an effective scavenger of ROS and free radicals (*i.e.* hydroxyl radical, superoxide anion, lipid peroxyl radical and hydrogen peroxide) either directly or indirectly through enzymatic reactions[131]. The presence of the sulfhydryl group on GSH plays a crucial role in the direct scavenging of ROS. With the one-electron transfer from the thiol moiety to the radical, an unstable GSH radical ($GS^{\cdot}$) is produced. The $GS^{\cdot}$ radical will bind rapidly with another to produce GSSG and a superoxide anion, in the presence of oxygen[131]. The superoxide anion is further detoxified by the enzyme superoxide dismutase (SOD). When SOD activity is reduced, GSH can promptly compensate, leading to the protection against oxidative stress and cell death[141,142]. One of the most important mechanisms for reducing and detoxifying hydrogen peroxide is the antioxidant function of GSH accomplished through the GSH peroxidase (GPx)-catalyzed reactions[131]. GPx1 is the major isoform and is localized in the mitochondrial matrix and the intermembrane space[125,143]. GPx1 has substrate specificity for hydrogen peroxide, and upon detoxification of hydrogen peroxide, GSH becomes oxidized. Furthermore, GSH acts as an antioxidant in the detoxification of products from oxidized lipids, such as malondialdehyde[144]. The function of GSH as an antioxidant is also involved in other primary antioxidant systems within the cell. Dehydroascorbate reductase relies on GSH to act as an

electron donor in the regeneration of ascorbate from dehydroascorbate, the oxidized product[145]. The function of GSH is multifaceted, with a major role in the elimination of toxins that are normally produced during cellular metabolism.

1.4. Glutaredoxin System

The glutaredoxin (glutathione dependent reductase and oxidase; *Grx*) system was first discovered in 1976[146] and exists in most living organisms including prokaryotes[146], plants[147,148], viruses[149,150] and eukaryotes[151,152]. The glutaredoxins are small (9-14 kDa) abundant proteins that catalyze the exchange of thiol-disulfide groups from oxidized protein disulfides and mixed disulfides[153]. Glutaredoxins belong to the oxidoredcutase family and play an important role in cellular redox-dependent processes. In the glutaredoxin system, electrons are transferred from NADPH via GR and GSH to one of the glutaredoxin isoforms and finally to the oxidized target (Fig. 1.4). When glutaredoxin reduces the target protein, the glutaredoxin protein becomes oxidized and is subsequently reduced by GSH.

1.4.1 Mammalian Glutaredoxin Isoforms

To date, there are four mammalian isoforms of glutaredoxins: glutaredoxin-1 (*Grx1*), glutaredoxin-2 (*Grx2*), glutaredoxin-3 (*Grx3*) and glutaredoxin-5 (*Grx5*)[154], all of which play crucial roles in maintaining cellular redox homeostasis. The four isoforms are divided into two groups based on their cysteine residues at the active site. The dithiol glutaredoxins, *Grx1* and *Grx2*, which have a CXXC

active site motif and a GSH binding site, and the monothiol glutaredoxins, *Grx3* and *Grx5*, which have a CXXS active site motif[155,154].

The 12 kDa *Grx1* is found at low levels (1 μM) within the cell[153] and has a Cys-Pro-Tyr-Cys motif[117]. It is primarily located in the cytosol, but can be translocated into the nucleus[156], secreted into the plasma[157] and has been found in the intermembrane space of mitochondria[158]. Studies have demonstrated that when the *Grx1* gene is knocked out of mice, there is a protective effect against inflammation[159] and cardiovascular hypertrophy[160]. This may suggest that the main role of *Grx1* is not necessarily as an antioxidant, but rather is involved in the reduction of protein mixed disulfides with GSH.

Grx2 is encoded by one gene but alternative splicing of the transcript renders one isoform that targets the nucleus and the other the mitochondrial matrix[161]. *Grx2* is widely expressed in many tissues with high levels in the heart, skeletal muscle, testis, and liver[162]. *Grx2*, an 18 kDa protein[163], shares approximately 34% sequence homology with *Grx1*[154]. However, the active site sequence of *Grx2*, Cys-Ser-Try-Cys, differs from that of *Grx1* by the serine amino acid. The replacement of proline with serine results in a greater affinity for the reduction of glutathionylated proteins[164]. *Grx2* catalyzes protein glutathionylation and deglutathionylation reactions and depends on changes in the GSH:GSSG ratio[165]; a high GSH:GSSG ratio promotes protein deglutathionylation and a low GSH:GSSG ratio promotes *Grx2* glutathionylase activty[165,166]. *Grx2* is also essential in cellular responses to

oxidative stress. For instance, when levels of mitochondrial *Grx2* were depleted in cultured human cells, cell sensitivity to apoptosis increased as a response to increased oxidative stress[167]. Furthermore, our laboratory has previously shown that *Grx2* controls the activity of uncoupling protein-3 (UCP3) through glutathionylation, and thereby controls UCP3-mediated proton leak in muscle mitochondria[168].

Although the monothiol glutaredoxins lack the C-terminal active site thiol, they are still capable of binding and utilizing GSH as a substrate[169]. *Grx3* is a 38 kDa monothiol with the active site Cys-Gly-Phe-Ser and is located in the cytosol and the nucleus[154]. *Grx3* is important for embryonic development and genetic ablation caused embryonic death[170]. *Grx5* is the other mammalian monothiol and shares the same active site of *Grx3*. The 17 kDa protein is evolutionarily conserved in eukaryotes and is located in the mitochondria[171]. *Grx5* does not exhibit disulfide reductase activity[154], but is involved in the maintenance of iron homeostasis[172]. Deficiency of *Grx5* results in altered cellular iron metabolism and production of heme[173,174]. Furthermore, *Grx5* has been shown to provide protection against oxidative stress and apoptosis[173].

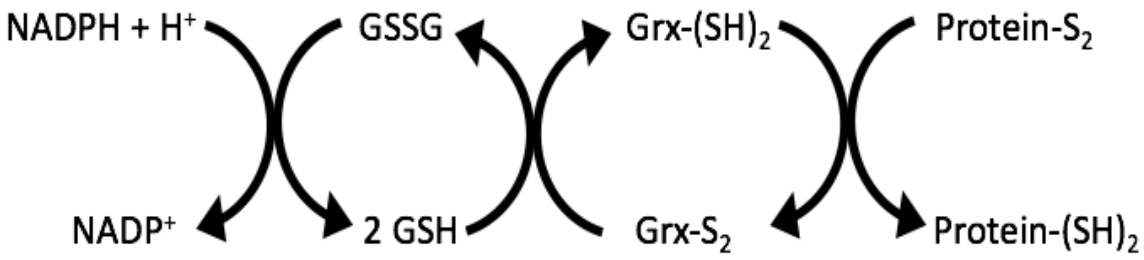

Figure 1.4. General diagram of the glutaredoxin system. In the glutaredoxin system, electrons are transferred from NADPH to GR, GSH and finally to one of the glutaredoxin isoforms. Subsequently, glutaredoxins will reduce disulfides in the target proteins.

1.4.2 De-/Glutathionylation Function of Glutaredoxin-2

Mitochondrial *Grx2* is a versatile oxidoreductase that plays a crucial role in mitochondrial redox homeostasis by catalyzing the reversible glutathionylation/deglutathionylation reactions[165,175]. Glutathionylation is a post-translational modification of protein thiols by the addition of GSH[176]. Proteins with cysteine residues are more susceptible to redox-dependent modifications during oxidative stres[169]. Thus, glutathionylation occurs mainly as a response to oxidative stress when GSH:GSSG is ~1[177]. Due to the high intra-mitochondrial GSH:GSSG ratio, glutathionylation is minimized under basal physiological conditions[122,178]. Since *Grx2* is not as easily inactivated by oxidants, it is able to function efficiently in oxidatively stressed mitochondria[165,179]. The interaction of protein thiols with the GSH pool is important for antioxidant defense and redox signaling[122,180]. When proteins are glutathionylated, specific functional changes (*i.e.* activation or deactivation) occur, which are important in regulating signaling processes[176]. Furthermore, glutathionylation serves as a protective mechanism for protein thiols from irreversible oxidation[181,182] and as a form of storage for GSH, to prevent loss of GSH during oxidative stress[176]. The thiol-disulfide exchange between the protein and GSH and the reverse reaction are relatively slow[183,184]. Therefore, *Grx2* is required to catalyze these reactions[185,186]. Proteins of the ETC are rich in protein thiols[187] and one of the main targets for *Grx2* in mitochondria are the proteins in

complex I[177,188]. These protein reactions are favored within the mitochondria due to the following characteristics: the alkalinity of the mitochondrial matrix ionizes protein thiols, which increases their reactivity toward GSH, the high amount of protein thiols and GSH present in the mitochondria (60-90mM and 5mM, respectively) and the production of ROS[189,190]. Glutathionylation of complex I has an inhibitory effect on its activity[191] and is associated with increased mitochondrial superoxide production[188]. Compared to the other respiratory complexes, complex I is more susceptible to glutathionylation and inactivation[188].

CHAPTER II: AIMS AND HYPOTHESIS

The overall aim of this thesis has been to investigate the effects of *Grx2* deficiency on GSH redox, mitochondrial structure and function in skeletal muscle. Intriguingly, cellular GSH redox has recently been shown to control mitochondrial fusion[119]. As discussed in Chapter I, Shutt *et al.*[119] demonstrated in an *in vitro* cellular system that increased levels of GSSG resulted in increased mitochondrial fusion. Furthermore, when *Grx2* was knocked down in mouse primary myotubes, proton leak was increased and GSH homeostasis was altered, with elevated levels of GSSG[168]. The overall hypothesis is that glutaredoxin-2 knockout ($Grx2^{-/-}$) mice will exhibit a decrease in the GSH ratio, in skeletal muscle, which will result in an increase in mitochondrial length and impaired mitochondrial function.

The specific objectives of the experimental studies were the following:

- To investigate, in skeletal muscle, how the GSH redox ratio impacts mitochondrial structure and function in the absence of glutaredoxin-2.
- To provide a possible mechanism explaining the disordered skeletal muscle mitochondrial ultrastructure and energetics in the $Grx2^{-/-}$ mice.
- To examine whether the GSH redox ratio affects levels of autophagy and mitophagy markers in $Grx2^{-/-}$ skeletal muscle.

CHAPTER III: MATERIALS AND METHODS

Animals

All experimental procedures that involved the use of mice were conducted as per the guidelines and principles of the Canadian Council of Animal Care. The experiments were performed after the approval of the Animal Care Committee of the University of Ottawa. Studies were conducted on male C57BL/6 mice wild-type and *Grx2* whole body knock-out mie aged 4 to 6 weeks. PCR was conducted on all mice prior to experiments to confirm the knock-out of *Grx2*. All mice were housed in the same room under standard conditions (20-22ºC, 55-65% humidity) and subjected to a 12 hour light/dark cycle of (Light: 06:00-18:00). Mice were fed a standard chow diet (58% kcal from carbohydrate, 18% from fat and 24% from crude protein; 2018 Teklad Global Rodent Diet, Envigo) and food and water were provided *ad libitum*. For all experiments, mice were sacrificed at 4-6 weeks of age.

Body Composition

Fat and lean mass were measured by a nuclear magnetic resonance imaging whole-body composition analyzer (EchoMRI-700™; Echo Medical Systems, Houston, Texas). This was a non-invasive method was performed on conscious mice.

Indirect Calorimetry

Energy expenditure, (*i.e.* O_2 consumption), as well as CO_2 production, respiratory exchange ratio (RER: VCO_2/VO_2), spontaneous and wheel-running activity and food intake were measured in a 12 chamber Comprehensive Lab Animal Monitoring System (CLAMS) instrument (Columbus Instruments, Columbus, Ohio). Mice were individually housed in chambers and acclimated for 24-48 hours, before collection of 24h of data. The temperature of the unit was kept at 28-30ºC and mice were given free access to a standard diet (2018 Teklad Global Rodent Diet; Envigo) and water and were housed with the standard light-dark cycle (light 06:00-18:00 and dark 18:00-06:00). Mouse wheel-running activity was calculated as the total number of complete wheel rotations per day.

Tissue Collection and Preparation

Animals were culled by cervical dislocation. The *tibialis anterior* muscle was isolated from both limbs and immediately divided for different analyses. Tissues were weighed, and flash-frozen in liquid nitrogen or placed in ice cold BIOPS solution (see below) for use in respiration assays. All stored tissues were kept at -80ºC until processed.

Mitochondrial Energetics in Permeabilized Muscle Fibers

Characteristics of the mitochondrial oxidative phosphorylation system were assessed in permeabilized muscle fibers prepared from *tibialis anterior* muscle. High-resolution respirometry was conducted using an Oxygraph-2k system (OROBOROS Instruments, Innsbruck, Austria). *Tibialis anterior* samples were placed in ice-cold relaxation medium (BIOPS) immediately after harvesting. BIOPS solution consisted of 50 mM K^+-MES, 20

mM taurine, 0.5 mM dithiothreitol, 6.56 mM $MgCl_2$, 5.77 mM ATP, 15 mM phosphocreatine, 20 mM imidazole, pH of 7.1 adjusted with 5 N KOH at 0°C and 10 mM Ca–EGTA buffer (2.77 mM CaK_2EGTA + 7.23 mM K_2EGTA; 0.1 mM free calcium)[192]. Muscle fibers were mechanically separated and permeabilized using freshly prepared saponin solution (50 µg/mL BIOPS; 5 mg of saponin/mL of BIOPS) on ice for 30 minutes. Fibers were then rinsed in mitochondrial respiration medium (MiR05)[192]. MiR05 consisted of 110 mM sucrose, 60 mM K^+-lactobionate, 0.5 mM EGTA, 3 mM $MgCl_2$, 20 mM taurine, 10 mM KH_2PO_4, 20 mM HEPES adjusted to pH 7.1 with KOH at 37 °C; and 1 g/l BSA essentially fatty acid free. Muscle fibers were then blotted and weighed using a microbalance (Mettler-Toledo XPE105) and placed into the respirometry chambers. Two separate protocols were used and experiments were performed at 37°C. The oxygen concentration during experiments was kept between 200 and 400 nmol/mL. The first protocol included consecutive additions of 2 mM malate, 5 mM pyruvate, 10 mM glutamate, 5 mM ADP (complex I- supported respiration), 10 mM succinate (complex I- and complex II- supported respiration), 0.25 µM titrations of carbonyl cyanide p-trifluoromethoxyphenyl hydrazine (FCCP) (maximal respiration), 2.5 µM antimycin A (AA) and 2 mM N,N,N',N'-Tetramethyl-p-phenylenediamine dihydrochloride (TMPD) with 2mM ascorbate (cytochrome *c* oxidase (COX) activity). The second protocol included successive additions of 2 mM malate, 200 µM octanoyl carnitine, 5mM ADP (fatty acid-supported respiration), 5 mM pyruvate, 10 mM glutamate, 10 mM succinate, 2.5 µM oligomycin (leak respiration). Values are corrected to non-mitochondrial oxygen consumption (AA).

Cell culture

Primary myoblasts from 4-6 week old WT and $Grx2^{-/-}$ mice were isolated from the *quadriceps, tibialis anterior, soleus and gastrocnemius* muscles. The pooled muscle groups were minced and treated with collagenase/dispase (C/D) (Collagenase: 0.1U/mL, Dispase: 0.8U/mL) solution to liberate myoblasts. The muscles were left in C/D solution for two 15-minute incubation periods, during which they were placed in a humidified incubator at 37°C in 5% CO_2. After each 15-minute incubation period, the solution was triturated about 20-25 times. Primary cell enrichment was achieved by employing the differential adhesion process, which involves repeated plating to remove fibroblast population, which rapidly adhere to culture flasks[193]. Myoblasts were cultured in Dulbecco's modified Eagle medium (DMEM) containing 20% bovine growth serum (BGS), 1% Antibiotic-Antimycotic (AA), 30 ng/μL basic fibroblast growth factor (bFGF) and 5μg/mL gentamycin sulfate.

Fluorescent Microscopy of Primary Myoblasts

Upon 85-90% confluency, cells were trypsinized and plated for imaging. Myoblasts were placed in starvation medium (SM) for an incubation period of 14-16 hours prior to cell fixation; starvation was used to synchronize cell cycle and reach a quiescent state (G_0 state). The SM consisted of DMEM supplemented with 0.1% BSA and 1% AA. After the starvation period, cells were fixed with 4% paraformaldehyde for 15 minutes. The cells were permeabilized and blocked using a blocking buffer containing 0.1% Triton X-100 and 1% BSA, which also included the primary antibody rabbit TOMM20 (Santa Cruz Biotechnology, sc-11415; 200 μg/ml) in a 1/100 concentration. Secondary antibody

Oregon green 488 goat anti-rabbit (Life technologies, O-6381; 2 mg/mL) was used in a 1:100 dilution in 1x PBS. Hoechst counter-stain was also included in the secondary antibody solution. Images were obtained using the Zeiss Axiolmager M2 epifluorescent upright microscope with a Plan-Apochromat 63X/1.4 oil objective.

Sample/Lysate Preparation for Western Blot

Approximately 20-30 mg of *tibialis anterior* muscle was weighed and minced into smaller pieces with a blade. Minced pieces were placed into a glass tube containing lysis buffer (1000 µL/50 mg) [10 mM TRIS HCl (pH 7.4), 150 mM NaCl, 1 mM EDTA, 0.5% Triton] with protease/phosphatase inhibitor cocktail (88669; Thermo Scientific). A Potter-Elvehjem pestle was attached to an electric drill and placed into homogenization tube. The drill was set to 120V for 10 strokes, followed by 140V for another 10 strokes. The homogenate was then transferred into a minitube and vortexed for approximately 10 seconds. The lysates were centrifuged at 10,000g for 10 minutes at 4ºC. The resulting supernatant was collected and stored at -80ºC for future experiments.

Transmission Electron Microscopy

Transmission electron microscopy (TEM) was used to examine mitochondrial structure in WT and $Grx2^{-/-}$ *tibialis anterior* muscle. In brief, muscle samples were fixed in 2.5% glutaraldehyde in a 0.1 M sodium cacodylate buffer. The cell suspension was further fixed in an OsO_4 (2%) in a 0.1 M sodium cacodylate buffer. After washing in a 0.1 M sodium cacodylate buffer, the cells were dehydrated in a growing series of alcohol. The most concentrated alcohol was replaced with acetone. The material was penetrated by a growing

series of Araldite diluted in acetone. Finally, the tissues were embedded in Araldite (Huntsman Advanced Materials LLC, United States). Ultrathin sections (80 nm) were prepared using an Ultracut Leica UC6 ultramicrotome (Leica Microsystems, Germany) and placed onto a copper grid coated with formvar film. Sections were stained with uranyl acetate and lead citrate solutions and examined using a JEOL 1230 transmission electron microscope (JEOL JEM 1230, Tokyo). 55 micrographs were examined from each genotype at a magnification of 3,000. Mitochondrial volume density was estimated using the point counting method[194]. For each group, average volume density was calculated and the mean of the values was used[194].

Mitochondrial and Nuclear DNA Preparations

For determination of mitochondrial to nuclear DNA ratio, approximately 20 mg of *tibialis anterior* muscle was isolated. Muscle was placed in a sterile 2 mL centrifuge tube with 0.6 mL lysis buffer [10 mM Tris-HCl (pH 8.0), 1 mM EDTA and 0.1% SDS] and homogenized with a Dounce homogenizer with 20 strokes. 0.05-0.06 mL of 20mg/mL proteinase K (Invitrogen) solution was added and the lysates were incubated at 55ºC overnight. Lysates were vortexed vigorously and the non-soluble fraction was pelleted by centrifugation at 10,000 g for 15 minutes at room temperature. 0.6 mL of the supernatant was transferred to a new 2 mL tube containing 0.6 mL of phenol/chloroform/isoamyl alcohol (25:4:1) (PCIAA). Samples were vortexed and centrifuged at 10,000 g for 15 minutes. 0.45-0.5 mL of the supernatant was transferred to new 2 mL tube and equal volume of chloroform was added. The solution was vortexed and centrifuged at 10,000 g for 15 minutes. 0.4 mL of the supernatant was transferred to a new tube and mixed with 0.04 mL of 3mM NaAc

(Sigma) and 0.44 mL of isopropanol. The tube was kept at -20ºC for 10-30 minutes and then centrifuged at 10,000 g for 15 minutes to pellet the DNA. The resulting supernatant was discarded and the DNA pellet was washed twice with 0.5 mL of 70% ethanol, air dried and dissolved in 0.05 mL of nuclease free water.

DNA Concentration Determinations

Concentrations of mtDNA and nDNA were measured using Nanodrop 2000 spectrophotometer (Thermo Scientific). 10 ng/μL of genomic DNA stocks was used for qPCR amplification of mitochondrial encoded cytochrome c oxidase subunit I (CO1) and nuclear encoded Ndufv1. The CO1 primer sequences were 5-TGC TAG CCG CAG GCA TTA C-3 (forward primer) and 5-GGG TGC CCA AAG AAT CAG AAC-3 (reverse primer). The NDUFV1 primers were 5-CTT CCC CAC TGG CCT CAA G-3 (forward primer) and 5-CCA AAA CCC AGT GAT CCA GC-3 (reverse primer)[195]. For PCR sample preparation, 1 μL of genomic DNA was mixed with 1 μL of each primer (10 μM), 3 μL of nuclease-free water and 5 μL of SYBG master mix. The reaction was initiated at 94ºC for 10 minutes, followed by 40 cycles through 94ºC x 10s, 60ºC x 30s and 94ºC x 10s. All reactions were run in duplicates. Amplification curves were analyzed using SDS 1.9.1 software and curves were used to determine relative mtDNA:nDNA ratio.

GSH and GSSG Determinations Using High-Performance Liquid Chromatography (HPLC)

Concentrations of GSH and GSSG were determined by HPLC using an Agilent 1100 Series instrument, equipped with a Pursuit 5 C_{18} column (Agilent Technologies) with a flow rate

set to 1mL/min. The mobile phase [10% methanol, HPLC plus (Sigma, 646377-4L), 90% ddH_2O, 0.09% trifluoroacetic acid (Sigma, 302031-100 mL)] was filtered using a 0.22 μm filter. Experiments were performed on 85-90% confluent myoblasts from two 75 cm^2 flasks. Twenty-four hours prior to the experiment, the cells were subjected to serum deprivation to synchronize cells into a state of quiescence[196]. The following day, cells were trypsinized and centrifuged at 300 g. The supernatant was discarded and the pelleted cells were washed twice in cold 1X phosphate-buffered saline (PBS) solution. Following the second PBS wash, cells were re-suspended in 440 μL of cold 1X PBS and 40 μL of cell solution was taken for cell count using the Cell Countess (Thermo Fisher Scientific). The cells were subsequently centrifuged at 300 g and the supernatant was removed, and the pellet was re-suspended in 1:1 buffer [1% (v/v) trifluoroacetic acid (Sigma, 302031-100 mL) and 1% (w/v) meta-phosphoric acid (Sigma, 239275-5G) solution in mobile phase and homogenization buffer (for 25 mL, 2.14 g sucrose, 30.3 mg TRIS, 21.9 mg EDTA dissolved in mobile phase, pH of 7.4)] and incubated on ice for 20 minutes. The solution was then transferred to a new tube and centrifuged at 14,000 g for 20 minutes at 4°C. After centrifugation, the supernatant was collected and subjected to HPLC. GSH and GSSG were detected using the Agilent UV-visible wavelength detector at 215 nm. Retention times were confirmed via standards, which were prepared using 0.01mM and 0.1mM of GSH (Sigma, G4251) and GSSG (Sigma, G4501) dissolved in 1:1 buffer. Absolute amounts of GSH and GSSG were determined by calculating the area under the respective peaks in the chromatogram.

Bradford Assay for *Protein Quantification*

Protein content for each sample was determined using a Bradford protein assay and a BSA standard curve; results were read by a microplate reader (SynergyMX; BioTek, Winooski, VT). 1X Bradford protein assay reagent (BioRad, Mississauga, ON) was prepared and added to standards and samples. The software Gen5 (BioTek, Winooski, VT) was used to record the absorbance values at 595 nm.

Western Blot for Autophagy/Mitophagy Markers

Sample aliquots were suspended in Sample Buffer (SB; 1.5 mL of 1 M Tris-HCl pH of 6.8, 3 mL of 1 M dithiothreitol, 0.6 g of sodium dodecyl sulfate, 0.03 g of bromophenol blue, 2.4 mL of glycerol, with a final volume of 7.5 mL), boiled at 95ºC for 5-10 minutes and centrifuged briefly. The samples were then loaded onto a gel (6-8% gradient gel) and 10 μL (1.76 μg) of the samples were loaded. Gel ran at 75V for 25 minutes then increased to 150V until the dye ran to the bottom of the gel. Membrane was transferred using a Trans-Blot Turbo (Bio-Rad). Four filter papers were soaked in Semi-Trans Buffer (48 mM Tris, 20 mM HEPES, 1.0 mM EDTA, 1.3 mM sodium bisulfite and 1.3 mM N,N-dimethylformamide (12.9 M for 99.8% purity)) then placed onto a tray. PVDF membrane, which was activated in methanol and in Semi-Trans Buffer, was added followed by the gel, then four additional pre-soaked filter papers were placed on top. Membranes were incubated with 5% milk blocking buffer (1.25 g of milk powder in 25 mL Tris buffered saline/0.1% Tween 20 (TBS-T)) for 1 hour at room temperature on a shaker. Membranes were rinsed and washed 3-5 times (5 minutes each) with 1X TBS-T. Membranes were then incubated with primary antibodies in 5% bovine serum albumin (BSA) buffer overnight at

4ºC under gentle agitation. Samples were probed for the following: p62 (1:3000, GP62-C; Progen), pACC (1:1000, 11818; Cell Signaling), pS6K (1:1000, 9205S; Cell Signaling), p4E-BP1 (1:1000, 2855; Cell Signaling), pGSK3beta (1:2000, 5558; Cell Signaling) and Parkin (Prk8) (1:5000, 808501; BioLegend). Membranes were rinsed and washed 5 times with 1X TBS-T at room temperature and probed with secondary antibodies in 2% milk (w/v) at room temperature for 1-2 hours. Membranes were then washed for 25 minutes in TBS-T and protein bands were visualized using ECL Immobilon Western Chemiluminescent HRP substrate (WBKLS0500; Millipore). Signals were captured using a ChemiDoc™ MP Imaging System (Bio-Rad). The following loading control were used: Vinculin (1:20000, V9131; Sigma).

Statistical Analysis

Statistical analysis was performed and graphs were generated using Prism software (GraphPad Software Inc., La Jolla, CA, USA). Statistical significance was determined using unpaired t-test comparing both genotypes. Data are expressed as mean ± SEM and a probability of $p<0.05$ was accepted as statistically significant.

CHAPTER IV: RESULTS

4.1 Physical and Metabolic Characteristics

Previously, our laboratory demonstrated that $Grx2^{-/-}$ mice aged 9-12 weeks exhibit a normal linear growth with no differences in liver, skeletal muscle and brown adipose tissue weights[197]. The first objective was to investigate the whole body metabolic phenotype in younger $Grx2^{-/-}$ mice (4-6 weeks). Body weights and body composition (Echo-MRI) quantification showed that total body weight and lean mass were slightly lower in the $Grx2^{-/-}$ compared to wild-type ($Grx2^{+/+}$) mice (*P*-values of 0.0022 for body weight and 0.0075 for lean mass comparisons; Fig. 2A, B). There were no differences in fat mass between the two genotypes, as determined by Echo-MRI (Fig. 2C). Food intake was measured using CLAMS, and did not differ between genotypes (Fig. 2D). The respiratory exchange ratio (RER; VCO_2/VO_2), which indicates the relative proportion of fuels being oxidized at the whole-body level (*i.e.,* carbohydrates vs. fats) was also determined. Between the two genotypes, the RER was relatively similar (Fig. 2E).

VO_2 levels normalized to lean body mass, were not different between wild-type (WT) or $Grx2^{-/-}$ mice (Fig. 2F). Activity levels, which were determined by complete wheel rotations, did not differ between genotypes (Fig. 2G).

4.2 Mitochondrial Respiration

Since our previous investigations into the effects of *Grx2* deficiency on mitochondrial energetics were conducted only in isolated mitochondria[168,197], we decided to assess characteristics of mitochondrial energetics in permeabilized muscle fibers. Thus, the sarcolemma was permeabilized and mitochondrial OXPHOS was examined *in situ* using high resolution repirometry. Specifically, we assessed characteristics of the OXPHOS system through the successive additions of specific substrates and inhibitors for the five major complexes of OXPHOS. Complex I was measured via the addition of malate, pyruvate and glutamate, which feed into the TCA cycle to produce NADH + H, which is then used by CI to drive OXPHOS. Similarly, complex II (succinate dehydrogenase) was measured via the addition of succinate, which is a direct substrate for CII. Complex IV was then measured by the addition of TMPD, which is used to reduce cytochrome *c* within CIV. These results demonstrate impaired CI activity in $Grx2^{-/-}$ permeabilized myofibers, as evidenced by the decreased in glutamate (glu)-driven respiration (Fig. 3A). There were no differences in CII or CIV driven respiration rates. Furthermore, maximal respiration, measured by the addition of the uncoupler FCCP (F), was not different between genotypes. Moreover, to determine if there were OXPHOS defects when respiration was fueled by fatty acid oxidation (FAO), we used a separate protocol using octanoyl carnitine as an energy substrate in additional samples of myofibers. Consistent with the previous protocol, results demonstrated impaired CI activity under these conditions as well. (Fig. 3B).

4.3 Mitochondrial Ultrastructure

Given that mitochondria exist as reticular networks in cells, and that *in vitro* studies suggest a role for GSH redox in the control of mitochondrial structure[119], we then examined mitochondrial structural characteristics and content in skeletal muscle tissue using transmission electron microscopy (TEM). We conducted these and subsequent analyses in *tibialis anterior* muscles. Electron micrographs showed that mitochondrial morphology is markedly abnormal in the Grx2$^{-/-}$ muscle (Fig. 4A-H). In wild-type muscle mitochondria cristae were found to be well-defined, and tubular (Fig. 4B, D). Whereas, micrographs showed that Grx2$^{-/-}$ mitochondria are frequently lacking in ordered cristae (Fig. 4F) and had unusual vacuole-like structures with double membranes (Fig. 4H). It also appeared that there were fewer mitochondria in the muscle. Thus, we used quantitative morphometry to determine mitochondrial content within the muscle. Quantitative morphometric analyses of 55 micrographs in each genotype revealed that mitochondrial content in the Grx2$^{-/-}$ muscle was less than half that in the WT skeletal muscle (Fig. 4I). We then sought to confirm these findings by using a common proxy method to measure mitochondrial content, the ratio of mitochondrial DNA to nuclear DNA (mtDNA: nDNA). However, there was no difference in mtDNA:nDNA between the two genotypes (Fig. 4J).

4.4 Mitochondrial Length

Given the previously published role of GSH redox on mitochondrial fusion in HeLa cells and mouse embryonic fibroblasts (MEFs)[119], our previous findings of lower mitochondrial GSH:GSSG in isolated mitochondria from Grx2$^{-/-}$ muscle[168] and our above-described findings of disordered mitochondrial ultrastructure, we hypothesized that the length of mitochondria in primary muscle cells of Grx2$^{-/-}$ mice would be increased compared to WT. To investigate a role for *Grx2* in mitochondrial fusion we used immunocytochemistry and subsequent quantitative morphometric analyses of TOMM20-stained primary myoblasts from both genotypes. Results showed that mitochondria length was increased, which can be indicative of increased fusion events (Fig. 5A-C).

4.5 Glutathione Concentrations

To determine if there were corresponding changes in GSH redox, we used high-performance liquid chromatography, to assess GSH and GSSG levels in WT and Grx2$^{-/-}$ primary myoblasts. Findings revealed that Grx2$^{-/-}$ myoblasts had a significantly decreased GSH redox ratio when compared to their WT counterpart (Fig. 6A).

4.6 Autophagy

Due to the irregular ultrastructure of mitochondria and the unusual membranous inclusions in Grx2$^{-/-}$ skeletal muscle, we hypothesized that autophagy could be affected in the absence of *Grx2*. Indeed, the ultrastructural analyses distinctly revealed ribosomes in the abnormal mitochondria (Fig. 7A, B), which could be indicative of autophagosomes in the Grx2$^{-/-}$ muscle. Redox signaling has been implicated in autophagy[198], and our previous research has shown impaired muscle mitochondrial GSH redox in Grx2$^{-/-}$ mice[168]. Thus, we investigated markers of autophagy in *tibialis anterior* muscle of Grx2$^{-/-}$ and WT mice aged 4-6 weeks. Commonly used markers include mammalian target of rapamycin complex 1 (mTORC1) and AMP-activated protein kinase (AMPK). The inhibitory function of mTORC1 induces autophagy by regulating the activity of the protein kinase ULK, which is required for autophagosome formation[199]. AMPK is thought to promote autophagy by inhibiting mTORC1 and the role of AMPK in autophagy in skeletal muscle is particularly important[200]. Western blot analyses revealed no differences in phosphorylated 4E-BP1 (target of mTORC1) or in phosphorylated ACC (target of AMPK) levels in Grx2$^{-/-}$ muscle (Fig. 7C). Furthermore, p62 levels were not different between genotypes, which would be indicative of autophagic flux.

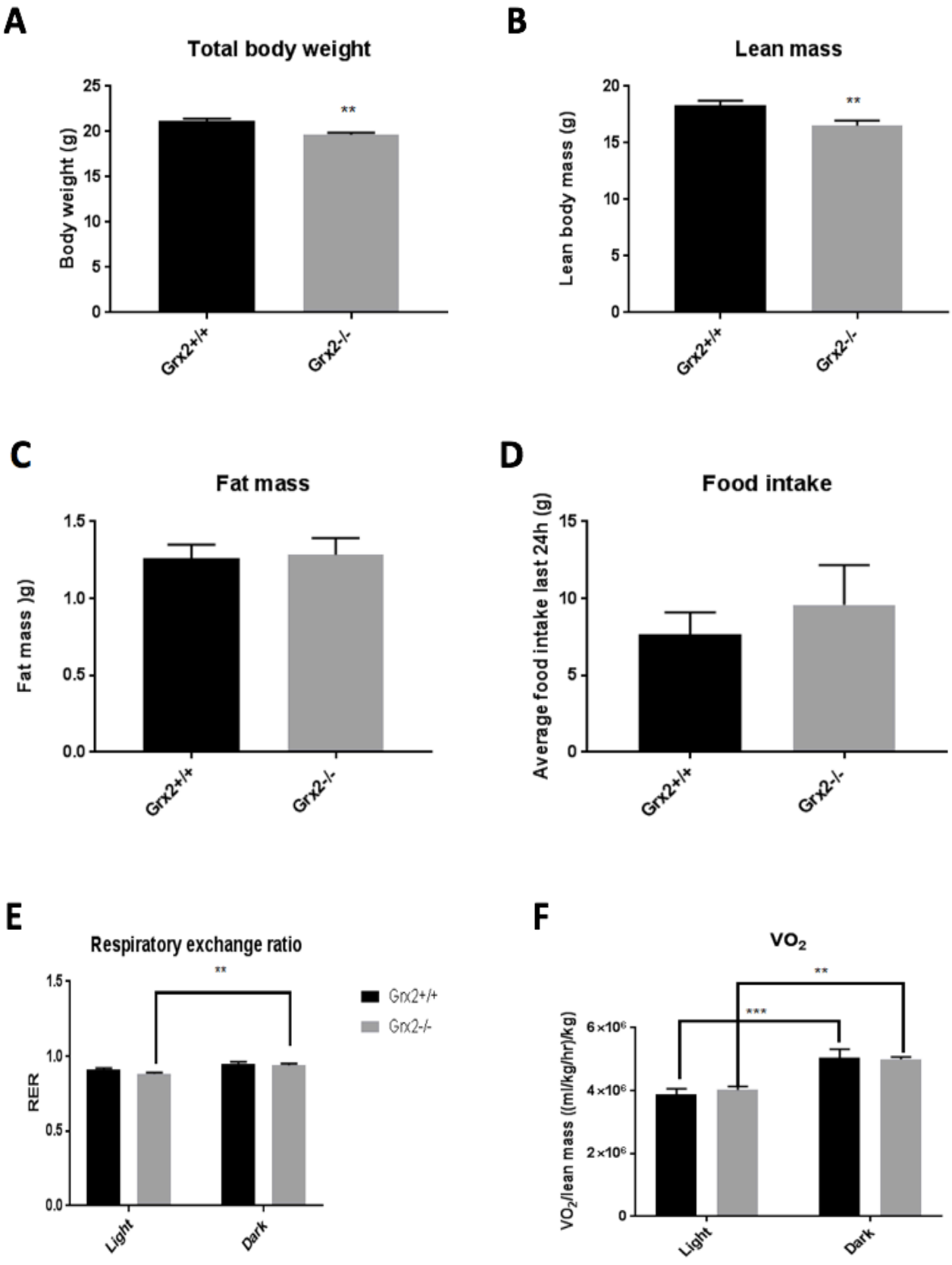
A
Total body weight
Body weight (g)
25
20
15
10
5
0
**
Grx2+/+
Grx2-/-
B
Lean mass
Lean body mass (g)
20
15
10
5
0
**
Grx2+/+
Grx2-/-
C
Fat mass
Fat mass)g)
1.5
1.0
0.5
0.0
Grx2+/+
Grx2-/-
D
Food intake
Average food intake last 24h (g)
15
10
5
0
Grx2+/+
Grx2-/-
E
Respiratory exchange ratio
**
RER
1.5
1.0
0.5
0.0
Grx2+/+
Grx2-/-
Light
Dark
F
VO2
**
***
VO2/lean mass ((ml/kg/hr)/kg)
6×10^6
4×10^6
2×10^6
0
Light
Dark

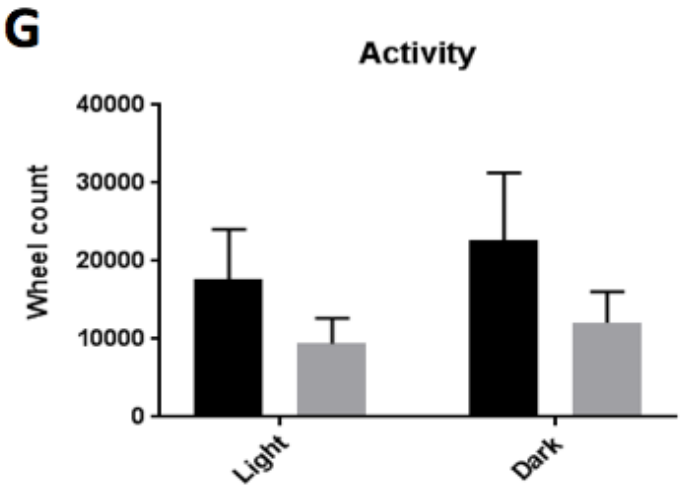

Figure 2: CLAMS performed in Grx2$^{+/+}$ and Grx2$^{-/-}$ showed differences in lean muscle mass and muscle weights.

(A) Total body weight and **(B)** lean mass are reduced in the Grx2$^{-/-}$ mice. **(C)** Fat mass and **(D)** food intake are not different between genotypes. **(E)** Grx2$^{+/+}$ and Grx2$^{-/-}$ mice have similar respiratory exchange ratios (RER). **(F)** VO_2 does not change between genotypes during the light or dark cycles. **(G)** Wheel count showed no differences in activity levels between genotypes. Data are mean ± SEM (n=11 for each genotype). $^{**}P<0.01$ $^{***}P<0.005$ vs. Grx2$^{+/+}$.

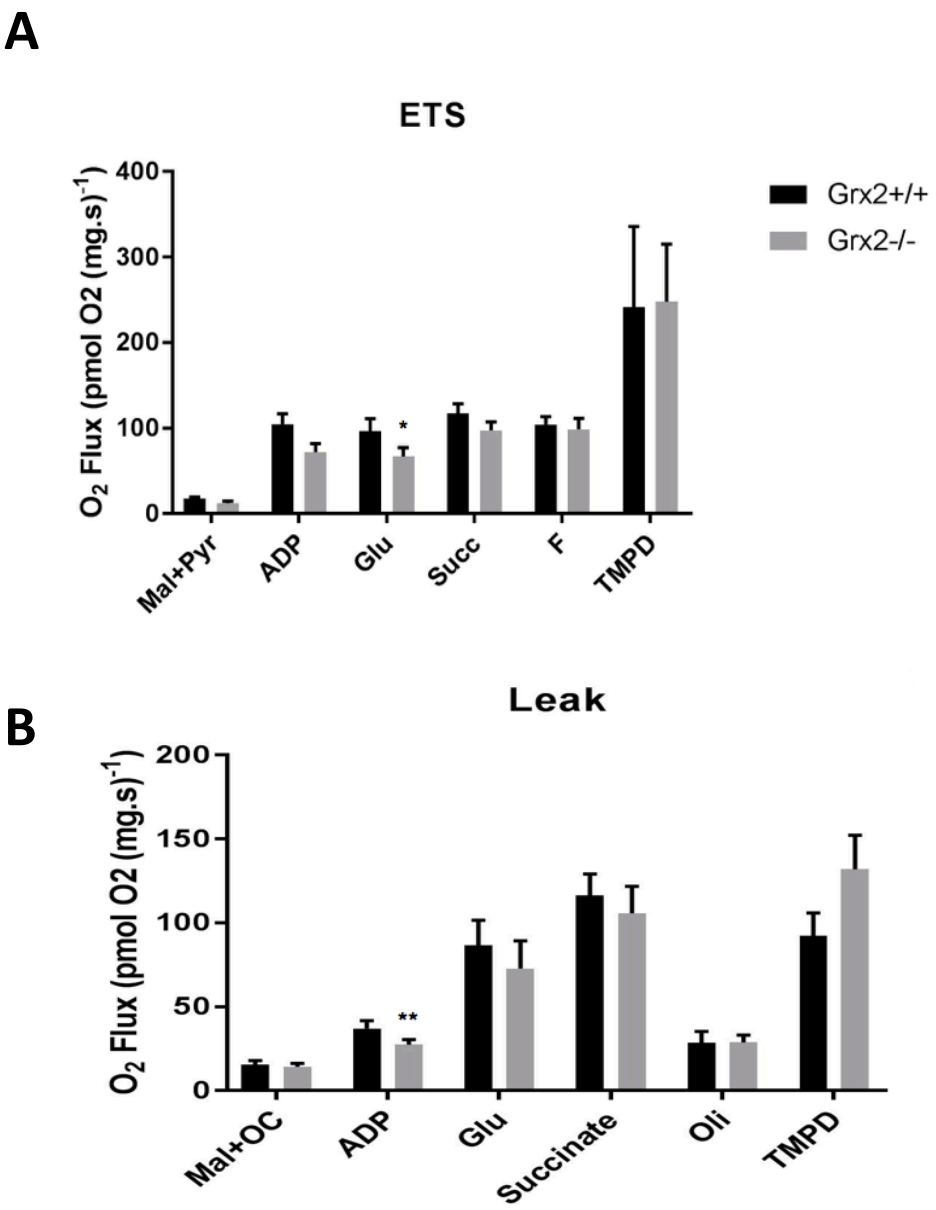

Figure 3: Mitochondrial energetics using high-resolution respirometry.

A) Respirometry data shows that complex I (CI) activity is impaired in $Grx2^{-/-}$ skeletal muscle. **(B)** CI activity, including the FAO substrate octanoyl carnitine, is also impaired, which is evidenced by the decrease after the addition of ADP. The electron transfer system (ETS) protocol includes substrates to stimulate OXPHOS; the leak protocol promotes proton leak with the addition of octanoyl carnitine and oligomycin.
Mal: malate, OC: octanoyl carnitine, Pyr: pyruvate, ADP: adenosine diphosphate, Glu: glutamate, Succ: succinate, F: FCCP, Oli: Oligo, TMPD: N,N,N',N'-Tetramethly-p-phenylenediamine dihydrochloride. Data are mean ± SEM (n=6). **P*<0.05, ***P*<0.01 vs. $Grx2^{+/+}$.

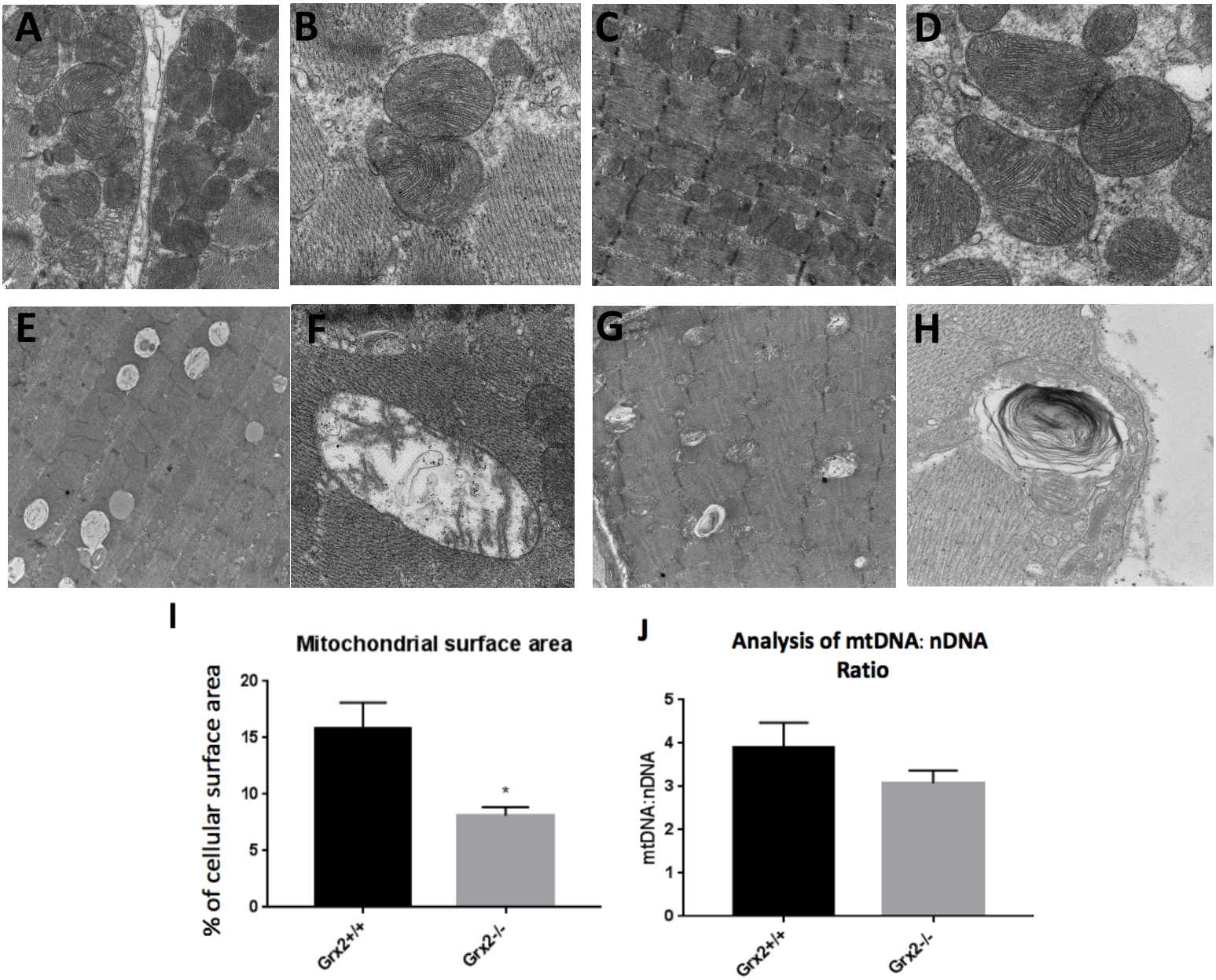

Figure 4: Electron micrographs show disordered mitochondrial morphology and a decrease in mitochondrial volume in Grx2^{-}/$^{-}$ skeletal muscle.

(A,C), **(E,G)** Representative images of Grx2^{+}/$^{+}$ and Grx2^{-}/$^{-}$ skeletal muscle, respectively; magnification of 3,000x. **(B,D)** Grx2^{+}/$^{+}$ *tibialis anterior* muscle displays well-defined cristae structures with normal mitochondrial shape; magnification of 10,000x and 12,000x, respectively. **(F,H)** In contrast, Grx2^{-}/$^{-}$ *Tibialis anterior* shows vacuole-like structures with double membrane, with abnormal cristae; magnification of 10,000x and 12,000x respectively. **(I)** Quantitative analyses of images shows a decrease in mitochondrial surface area. **(J)** No differences in the ratio of mtDNA to nDNA. Data are mean ± SEM (n=3 for TEM; n=6 mtDNA experiments). **P*<0.05 vs. Grx2^{+}/$^{+}$.

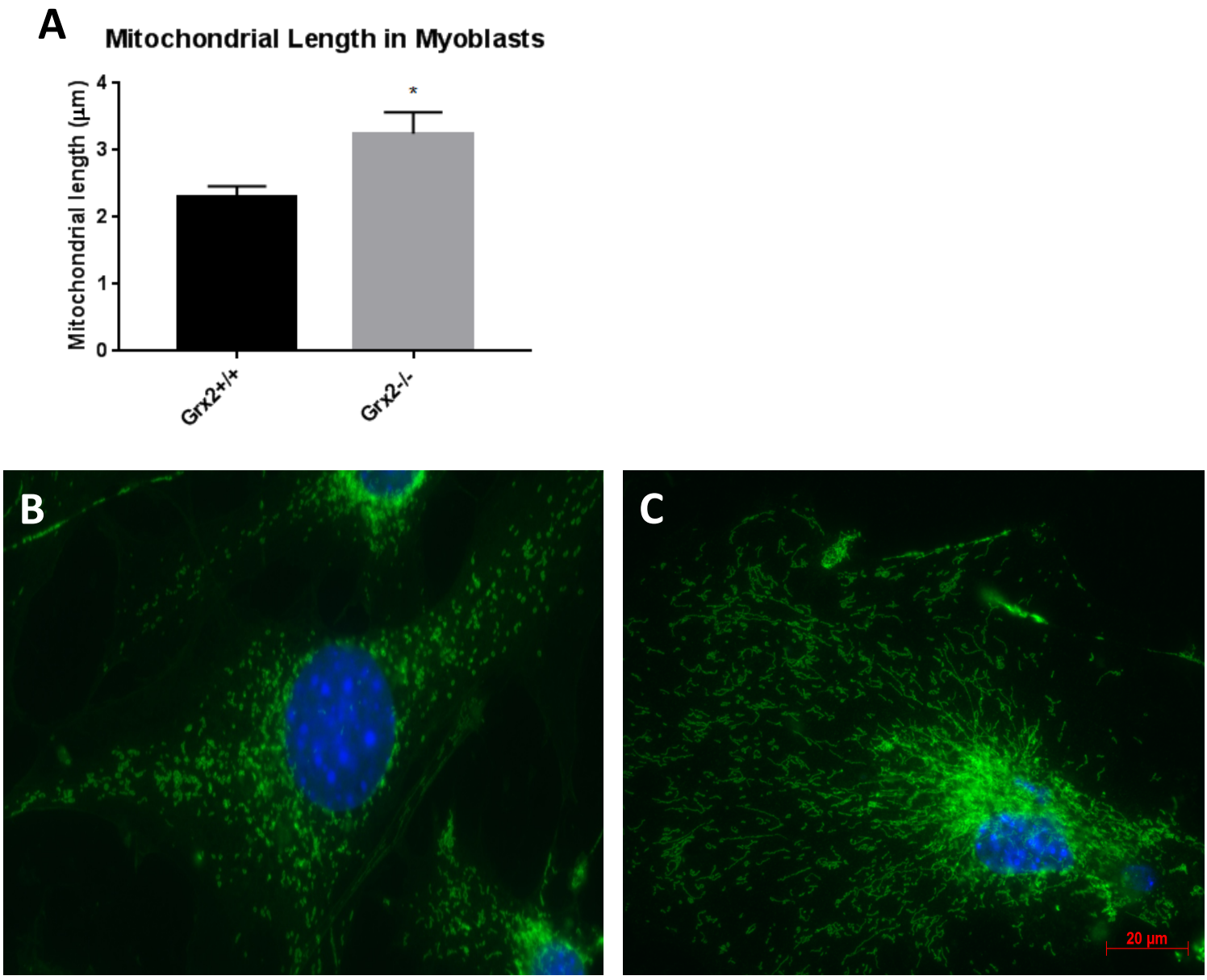

Figure 5: Mitochondrial length is increased in the* Grx2$^{-/-}$ *myoblasts.

A) Mitochondrial length is longer in Grx2$^{-/-}$ myoblasts. Representative images of **(B)** a Grx2$^{+/+}$ myoblast and **(C)** a Grx2$^{-/-}$ myoblast; scale bars, 20µm. Data are mean ± SEM (n=5 for immunocytochemistry). **P*<0.05 vs. Grx2$^{+/+}$.

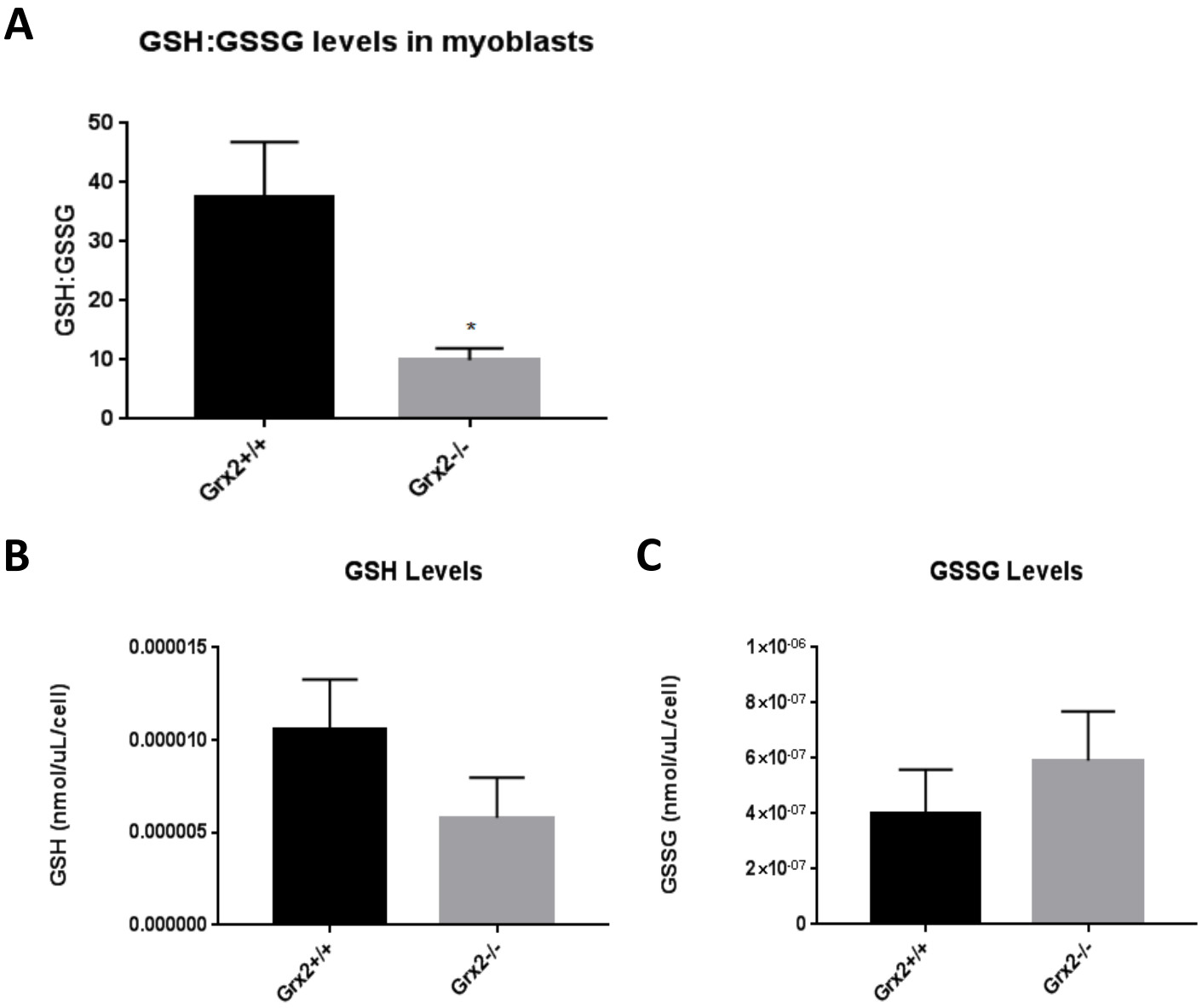

Figure 6: GSH:GSSG is decreased in the knockout myoblasts.

(A) Using HPLC, GSH:GSSG was found to be lowered in $Grx2^{-/-}$ myoblasts compared to their $Grx2^{+/+}$ myoblasts. **(B)** Absolute concentrations of GSH levels and **(C)** GSSG levels normalized to the number of cells. Data are mean ± SEM (n=6). **P*<0.05 vs. $Grx2^{+/+}$.

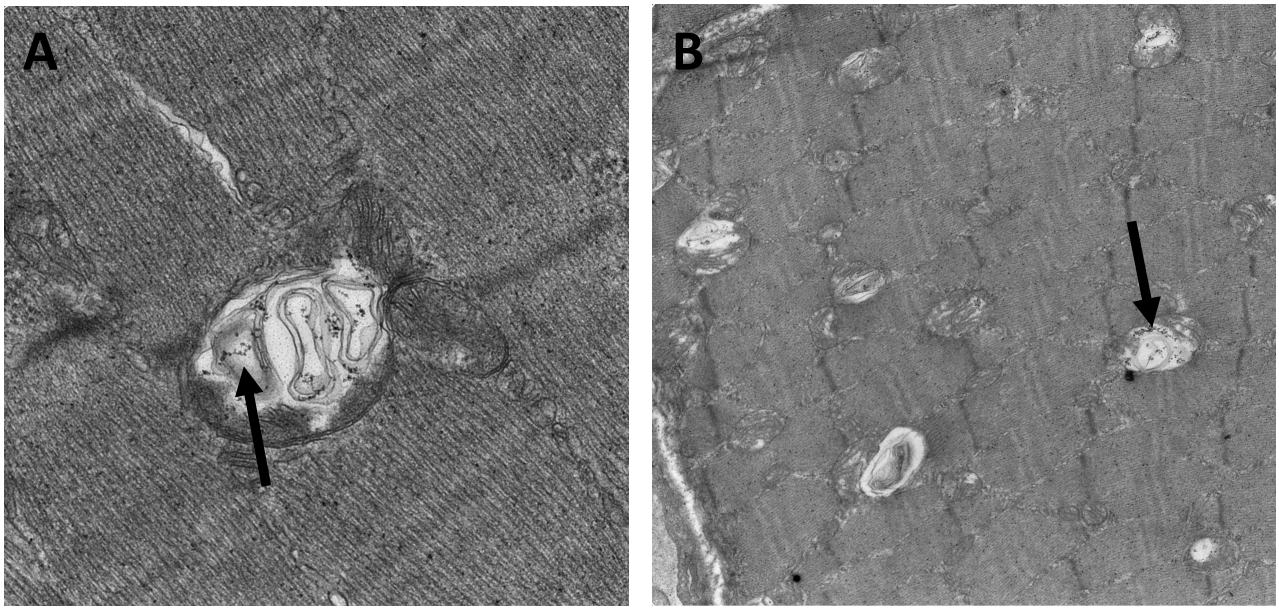

C

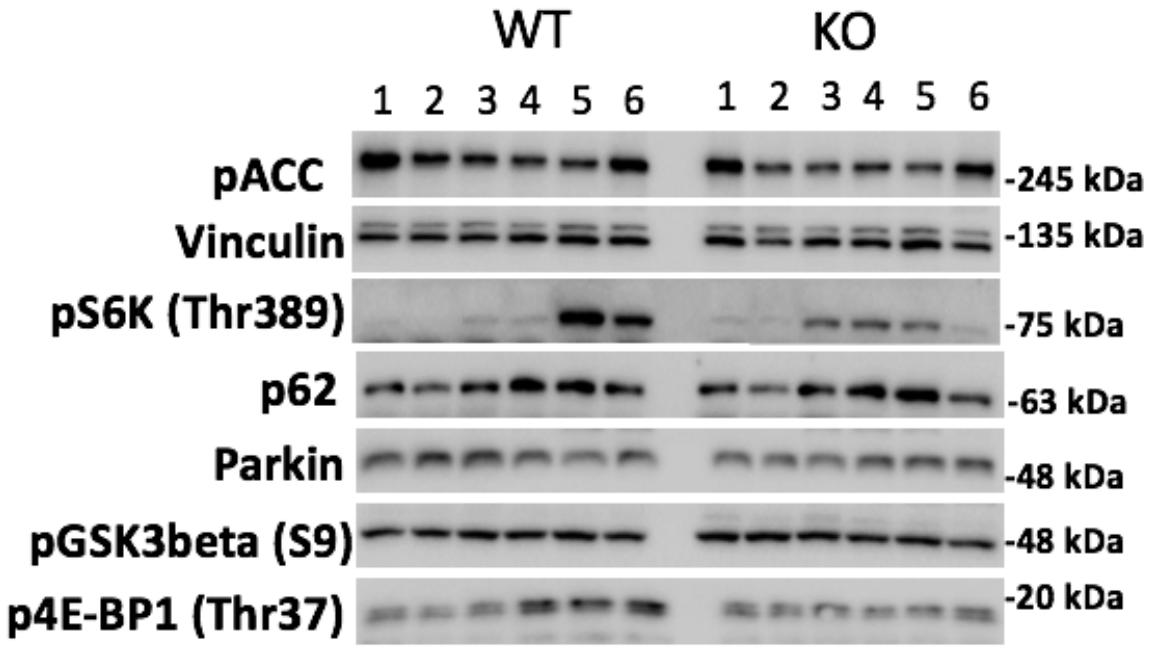

Figure 7: Grx2$^{-/-}$ skeletal muscle does not demonstrate autophagy impairment.

(A) and **(B)** Black arrows indicate ribosomes, which are indicative of autophagosomes. **(A)** magnified at 10,000x; **(B)** magnified at 3,000x. **(C)** Western blot of autophagy markers, mTOR and AMPK, does not indicate defects in autophagy. Data are mean ± SEM (n=3 for TEM; n=6 for WB). **P*<0.05 vs. Grx2$^{+/+}$.

CHAPTER V: DISCUSSION

This thesis provides the first-ever analyses of the effects of Grx2$^{-/-}$ on the structure and energetics of mitochondria *in situ* in muscle tissue and primary muscle cells. Previous studies have demonstrated that cellular GSH redox can affect the reticular structure of mitochondria[119], however the latter research was limited to analyses of immortalized cell lines (*i.e.* HeLa cells and MEFs) and the use of chemicals to alter GSH redox. Previous studies from our laboratory demonstrating altered mitochondrial GSH redox in muscle were also limited to isolated mitochondrial preparations[168,197], in which the reticular network of mitochondria that exists *in vivo* is damaged. Thus, this thesis aimed to study the effects of Grx2$^{-/-}$ on structural and functional aspects in mitochondria in intact tissue and cell systems.

To investigate the impact of a whole body *Grx2* knockout, indirect calorimetry and standard morphometrics were measured. Consistent with our previous findings in Grx2$^{-/-}$ mice aged 9-12 weeks[168], mice aged 4-6 weeks have a small yet significant decrease in total body weight compared to their WT counterpart. Grx2$^{-/-}$ mice used during this study possessed less lean mass compared to the WT mice, which was not previously shown in mice aged 9-12 weeks[168].

Mitochondrial content is an important factor that can limit oxidative capacity. To assess mitochondrial content, direct and indirect methods were used in the forms of TEM quantitative morphometry and mtDNA, respectively. While TEM quantitative morphometry demonstrated markedly lower mitochondrial content in Grx2$^{-/-}$ muscle, there was no difference in the ratio of mtDNA to nuclear DNA between genotypes. It is not

uncommon to obtain discrepant results between TEM and mtDNA measures of mitochondrial content. Morino *et al.* analyzed human muscle tissue from adults with or without a family history of type 2 diabetes, and found that decreases in mitochondrial content by TEM were not matched by any differences in mtDNA[201]. Within the context of the present study, there are a number of factors that could potentially explain the inconsistency between the results from the two different methods for assessing mitochondrial content. It is possible that mtDNA exists/is retained within the disrupted membranous structures that we observed in the micrographs of $Grx2^{-/-}$ muscle; this would have been measured in the mtDNA assays, but these disrupted structures would not have been identified as mitochondria in our morphometric analyses. Regardless, quantitative morphometry of images from TEM remain as the golden standard for measuring mitochondrial content[202], and our analyses revealed clear decreases in $Grx2^{-/-}$ muscle.

Mitochondrial fusion and fission are two distinctively important processes that affect mitochondrial structure and function in mammals[203,204,205]. Recently, mitochondrial fusion was shown to protect various parameters of mitochondrial function[203]. In skeletal muscle impaired mitochondrial fusion resulted in mtDNA mutations, possibly due to a decrease in mitochondrial content mixing, which normally allows for mtDNA genomes to complement one another[206]. In the current study, there was an increase in mitochondrial length in the $Grx2^{-/-}$ myoblasts compared to the WT myoblasts. This may be due to the observed differences in GSH redox (described below), and would be consistent with previously published *in vitro* analyses in transformed cells[119]. The perturbed GSH:GSSG ratio in the $Grx2^{-/-}$ myoblasts may cause the mitochondria to lengthen transiently to allow rapid mixing of contents and to maximize cellular energy production. While our observed

increase in mitochondrial length could be due to increased fusion events, it could be argued that there is impaired mitochondrial fission. Further investigations are needed to definitively identify the underlying mechanism of our observations (*e.g.* western blots of fusion and fission proteins and mitochondrial fusion assays).

Electron microscopy also revealed the presence of mitochondrial ultrastructural abnormalities, specifically in cristae number and structure. The cristae are invaginations of the mitochondrial inner membrane, where many of the OXPHOS protein complexes reside[40,41]. Since the cristae are major sites of OXPHOS[207], a positive correlation exists between the surface area of cristae and the levels of ATP produced during OXPHOS[208]. Cristae are functionally dynamic structures that remodel their shape in response to changes in cellular energy demands. For instance, when ADP levels are low, the cristae form a more 'condensed' structures[209]. Generally, any disruptions to the cristae structure will influence OXPHOS, thereby affecting cellular metabolism. The cristae in the $Grx2^{-/-}$ mitochondria were also disordered and it is possible that these structural impairments result in the observed impairments of CI activity. Furthermore, there is a strong correlation between mitochondrial content and cristae surface area because many of the mitochondrial proteins involved in OXPHOS reside within the cristae[202]. Although cristae surface area was not determined, the abnormal cristae structure observed in the $Grx2^{-/-}$ muscle could reflect a decrease in cristae surface area and, thus, would remain consistent with the reduced mitochondrial density.

Cristae remodeling is also implicated during the stages of apoptosis. Apoptosis, a programmed mode of cell death, is induced either by the mitochondrial intrinsic pathway or the extrinsic pathway. A study conducted by Scorrano and colleagues demonstrated that

after apoptosis was initiated, cristae structure was extensively remodeled, resulting in a substantial increase in cytochrome c release[210]. In the current study, we reasoned that the abnormal cristae remodeling structure could be indicative of disordered autophagy. Previous studies have visualized similar vacuole-like structures with multiple membranes and have been linked to autophagy[211]. The vacuole-like, double membranous structures seen in the $Grx2^{-/-}$ muscle further suggests the possibility that these structures are autophagosome-related vacuoles.

The intrinsic pathway of apoptosis involves the permeabilization of the MOM and the subsequent release of mitochondrial proteins (*i.e.* cytochrome *c*) from the intermembrane space[212,213]. *Grx2* can suppress apoptosis by preventing the loss of cardiolipin, the main phospholipid present in the mitochondrial inner membrane, and by inhibiting both the release of cytochrome *c* and the activation of caspase[167,175]. Moreover, the mitochondrial GSH pool seems to indirectly control the redox state of cardiolipin[214]. Thus, an increase in the peroxidized cardiolipin pool could accompany the observed decrease in GSH ratio, which can result in the permeabilization of MOM and release of cytochrome *c*. The GSH redox state in mitochondria is very reduced when compared to other organelles, (*i.e.* the nucleus and the endoplasmic reticulum)[215]. The GSH:GSSG ratio is an important indicator of redox environment[122,216] and changes in this ratio have been associated with apoptosis[217,218]. Specifically, a decrease in the GSH ratio is regarded as an early hallmark in the progression of apoptosis[219,220]. Furthermore, HeLa cells with silenced expression of *Grx2* by RNA interference experienced increased sensitivity to cell death induced by agents[167]. In contrast, overexpression of *Grx2* in HeLa cells reduces their sensitivity to apoptosis and prevents oxidation of cardiolipin[221]. Altogether, the literature

is consistent with the conclusion that *Grx2* provides a protective effect in apoptosis and thus, could expect an increased amount of apoptosis in the absence of *Grx2*.

When the mitochondrial GSH pool is depleted, an accumulation in hydrogen and lipid peroxides can occur in the mitochondria, thereby compromising mitochondrial function[125]. Furthermore, depletion of GSH has been shown to trigger the intrinsic mitochondrial pathways involved in autophagy, such as mitophagy[125,222]. Moreover, autophagy that was induced by trehalose (an autophagy inducer via non-mTOR pathway) was ameliorated with the addition of GSH[223]. These previous findings are consistent with the possibility that our observed decrease in GSH redox ratio in $Grx2^{-/-}$ myoblasts could have a potential effect on autophagy in the $Grx2^{-/-}$ muscle. Further experiments are required to focus on LC3-II and p62 markers in muscle homogenates and/or isolated mitochondria.

It is also notable that impaired autophagy has led to decreased levels of GSH[224]. We must also consider the possibility that if the $Grx2^{-/-}$ muscle does indeed demonstrate differences in autophagy markers, then changes in the GSH redox could be a result of impaired autophagy (*i.e.* in addition to the hypothesis that GSH redox causes changes in autophagy). When damages occur to a mitochondrion, the GSH pool becomes oxidized[188]. Since each mitochondrion has a distinct GSH redox state[225], the GSH:GSSG ratio could help distinguish the damaged mitochondria from the healthy mitochondria. Thus, the decrease in GSH:GSSG ratio in the $Grx2^{-/-}$ myoblasts could be indicative of a larger mitochondrial population damaged by the loss of *Grx2*.

Analyses of mitochondrial OXPHOS in permeabilized muscle fibers was conducted in this study, to detail mitochondrial functionality in intact mitochondria *in situ*.

Previous analyses by our lab were conducted in isolated mitochondria from skeletal muscle of Grx2$^{-/-}$ mice; results showed that *Grx2* is required to glutathionylate UCP3 and thus, inhibits UCP3-mediated proton leak[168]. Moreover, shGrx2 lentivirus was used to knockdown *Grx2* in mouse primary myotubes and the results demonstrated increases in proton leak[168]. In the current study of *tibialis anterior* myofibers from Grx2$^{-/-}$ and WT mice, impaired CI respiration was demonstrated, which is consistent with our previous findings of impaired CI respiration in isolated mitochondria. Since mitochondria do not export GSSG[226] (no transporters have been observed to date), elevated levels of GSSG appear to be sequestered in mitochondria, which may contribute to mitochondrial dysfunction by glutathionylation of target proteins[177] (*e.g.* complex I). Although the current study did not measure levels of glutathoinylated complex I in muscle, our lab has previously shown that the loss of *Grx2* in isolated mitochondria led to increased glutathionylation of complex I, which resulted in reduced OXPHOS activity[197]. Glutathionylation of complex I has also been associated with increased mitochondrial superoxide production[188], which would increase oxidation of GSH. Increased levels of GSSG, due to sustained glutathionylation of complex I proteins, could contribute to the destruction of the mitochondrion through autophagy[106] or contribute to excess mitochondrial damage and cell death[227]. There is a physiological relevance to the *Grx2*-catalyzed glutathionylation of complex I because of its central role in OXPHOS, but the details of this remain unclear. We also observed impaired myofiber respiration upon the provision of octanoyl carnitine, a substrate for FAO. However, FAO provides electrons at CI, CII and CIII of the ETC, so while these results are biologically meaningful, they do not specifically identify a given site of dysfunction in the ETC. Our findings did not

identify any differences in mitochondrial proton leak between genotypes, and thus do not confirm analyses conducted in myotubes in which *Grx2* was knocked down using siRNA[168]. This could be due to differences in experimental models (*e.g.* isolated mitochondria *vs.* intact fibers) and experimental conditions (*e.g.* differences in buffer compositions).

CHAPTER VI: FUTURE DIRECTIONS

The findings presented in this thesis provide insight into the impact of *Grx2* deficiency on mitochondrial structure and energetics. However, additional research is required to identify potential mechanisms underlying the disordered mitochondrial ultrastructure and function in the $Grx2^{-/-}$ muscle. It is suggested that the following experiments should be performed:

- To provide further insight into the changes in mitochondrial dynamics, a fusion assay should be performed on primary myoblasts as previously described[228]. Briefly, cells could be transfected with a mitochondrially-targeted photoactivable GFP (mtPAGFP) and a small region of the mitochondrial network is photoactivated. In this assay, the spread of the signal is recorded every 15 minutes for 1 hour using a time lapse confocal imaging system. Dilution of the signal intensity is equivalent to increased fusion events, thereby providing a quantitative measure for fusion rate.
- Since reduced mitochondrial membrane potential can result in mitochondrial fragmentation that target them for mitophagy, membrane potential should be measured. Along with the fusion assay, this experiment would help distinguish which process, either fusion or fission, is dominant in the $Grx2^{-/-}$ cells. Briefly, tetramethylrodamine ethyl ester (TMRE), would be used as a dye/fluorescent probe in live cells to quantify changes in membrane potential by fluorescence imaging.

TMRE, a positively-charged dye, accumulates in mitochondria in proportion to membrane potential due to the relative negative charge in the matrix. However, since mitochondrial fission usually generates depolarized mitochondria, these mitochondria would fail to sequester the TMRE dye.

- If there are changes in apoptotic events in the $Grx2^{-/-}$ muscle, (*i.e.* increased apoptosis), co-localization of mitochondria with autophagosomes should be performed. To measure mitochondrial sequestration by autophagosomes, mitochondria, from primary myoblasts, would be labeled with TOMM20 and RFP-Bnip3 and the autophagosomes would be labeled with GFP-LC3B[104]. Immunohistochemistry should also be performed in sections of *tibialis anterior* muscle.
- Since mitochondrial length was affected, it would be pertinent to investigate the proteins involved in both the fusion and fission processes. The following fusion proteins should be probed for via western blot: OPA1, Mfn 1 and Mfn2 and for fission proteins: Drp1, Fis1 and MFF.
- Autophagy proteins LC3-II and p62 should be blotted via western blots in isolated mitochondria from *tibialis anterior* muscle and in muscle tissue. These experiments will provide additional and distinct information regarding mitochondrial functionality and autophagy induction or inhibition.

CHAPTER VII: CONCLUSION

In conclusion, these findings are the first to demonstrate the importance of *Grx2* in maintenance of mitochondrial morphology and bioenergetics in intact mitochondrial networks of permeabilized muscle fiber preparations. Mitochondrial energetic analyses in myofiber preparations confirm impaired CI activity and reveal impaired fatty acid oxidation capacity. The highly irregular ultrastructure of mitochondria and abnormal membranous structures observed in electron micrographs of *tibialis anterior* muscle did not correlate with changes in major skeletal muscle autophagy markers (AMPK or mTOR), but more analyses are warranted.

GSH redox becomes disordered in aging and in many metabolic diseases, such as type 2 diabetes and obesity[229]. As GSH is one of the most important antioxidant defenses in cells, GSH depletion can result in increased sensitivity to oxidative stress[230]. Furthermore, several studies have demonstrated that GSH metabolism and transport are affected in type 2 diabetes, which inevitably alters the redox state of the cell[231,232,233]. Future research should examine the molecular mechanisms involved in a *Grx2* deficient model that leads to a decreased GSH ratio and abnormal mitochondrial morphology and function. It is important to design pharmacologically-based strategies that specifically target GSH synthesis, metabolism and transport, which could result in a potential therapeutic avenue for metabolic disorders.

REFERENCES

1. Frontera, W. R. & Ochala, J. Skeletal muscle: a brief review of structure and function. *Calcified tissue international* **96,** 183–195 (2015).
2. Jensen, J., Rustad, P. I., Kolnes, A. J. & Lai, Y. C. The role of skeletal muscle glycogen breakdown for regulation of insulin sensitivity by exercise. *Frontiers in Physiology* **2 DEC,** (2011).
3. Lang, B., Gray, M. & Burger, G. Mitochondrial Genome Evolution and the Origin of Eukaryotes. *Annu. Rev. Genet.* **33,** 351–397 (1999).
4. McBride, H. M., Neuspiel, M. & Wasiak, S. Mitochondria: More Than Just a Powerhouse. *Current Biology* **16,** (2006).
5. Nunnari, J. & Suomalainen, A. Mitochondria: In sickness and in health. *Cell* **148,** 1145–1159 (2012).
6. Wolfe, R. R. The underappreciated role of muscle in health and disease. *American Journal of Clinical Nutrition* **84,** 475–482 (2006).
7. Rasmussen, U. F. *et al.* Aerobic metabolism of human quadriceps muscle: in vivo data parallel measurements on isolated mitochondria. *Am. J. Physiol. Endocrinol. Metab.* **280,** E301–E307 (2001).
8. Kraegen, E. W. *et al.* Glucose transporters and in vivo glucose uptake in skeletal and cardiac muscle: fasting, insulin stimulation and immunoisolation studies of GLUT1 and GLUT4. *Biochem. J.* **295 (Pt 1,** 287–293 (1993).
9. Douen, A. G. *et al.* Exercise induces recruitment of the 'insulin-responsive glucose transporter': Evidence for distinct intracellular insulin- and exercise-recruitable

transporter pools in skeletal muscle. *J. Biol. Chem.* **265,** 13427–13430 (1990).

10. Mueckler, M. Family of glucose-transporter genes. Implications for glucose homeostasis and diabetes. *Diabetes* **39,** 6–11 (1990).
11. Richter, E. a & Hargreaves, M. Exercise, GLUT4, and skeletal muscle glucose uptake. *Physiol. Rev.* **93,** 993–1017 (2013).
12. Lund, S., Holman, G. D., Schmitz, O. & Pedersen, O. Contraction stimulates translocation of glucose transporter GLUT4 in skeletal muscle through a mechanism distinct from that of insulin. *Proc. Natl. Acad. Sci. U. S. A.* **92,** 5817–21 (1995).
13. Sahlin, K., Tonkonogi, M. & Söderlund, K. Energy supply and muscle fatigue in humans. in *Acta Physiologica Scandinavica* **162,** 261–266 (1998).
14. Johnson, L. N. The regulation of protein phosphorylation. *Biochem. Soc. Trans.* **37,** 627–641 (2009).
15. Westerblad, H., Bruton, J. D. & Katz, A. Skeletal muscle: Energy metabolism, fiber types, fatigue and adaptability. *Experimental Cell Research* **316,** 3093–3099 (2010).
16. Hinkle, P. C. & Yu, M. L. The phosphorus/oxygen ratio of mitochondrial oxidative phosphorylation. *J. Biol. Chem.* **254,** 2450–2455 (1979).
17. HILL, A. V & WOLEDGE, R. C. An examination of absolute values in myothermic measurements. *J. Physiol.* **162,** 311–333 (1962).
18. Bleich, H. L., Boro, E. S., Felig, P. & Wahren, J. Fuel Homeostasis in Exercise. *N. Engl. J. Med.* **293,** 1078–1084 (1975).
19. Sugden, M. C. & Holness, M. J. Recent advances in mechanisms regulating

glucose oxidation at the level of the pyruvate dehydrogenase complex by PDKs. *Am. J. Physiol. - Endocrinol. Metab.* **284,** E855–E862 (2003).

20. Krebs, H. A. Body size and tissue respiration. *Biochim. Biophys. Acta* **4,** 249–269 (1950).

21. Stanley, W. C. & Connett, R. J. Regulation of muscle carbohydrate metabolism during exercise. *FASEB J.* **5,** 2155–9 (1991).

22. Rizzuto, R., Bernardi, P. & Pozzan, T. Mitochondria as all-round players of the calcium game. *J. Physiol.* **529 Pt 1,** 37–47 (2000).

23. Duchen, M. R., Verkhratsky, A. & Muallem, S. Mitochondria and calcium in health and disease. *Cell Calcium* **44,** 1–5 (2008).

24. Kent, M. Oxford Reference: The Oxford Dictionary of Sports Science & Medicine. *Oxford University Press* (2007). Available at: http://www.oxfordreference.com.ergo.southwales.ac.uk/view/10.1093/acref/9780198568506.001.0001/acref-9780198568506-e-2562.

25. Schwerzmann, K., Hoppeler, H., Kayar, S. R. & Weibel, E. R. Oxidative capacity of muscle and mitochondria: correlation of physiological, biochemical, and morphometric characteristics. *Proc. Natl. Acad. Sci.* **86,** 1583–1587 (1989).

26. Nair, K. S. Aging muscle. in *American Journal of Clinical Nutrition* **81,** 953–963 (2005).

27. Hood, D. A. Invited Review: contractile activity-induced mitochondrial biogenesis in skeletal muscle. *J. Appl. Physiol.* **90,** 1159–1167 (2001).

28. Santiago, C. *et al.* Mitochondriogenesis genes and extreme longevity. *Rejuvenation Res.* **16,** 67–73 (2013).

29. Berger, J. & Moller, D. E. The Mechanisms of Action of PPARs. *Annu. Rev. Med.* **53,** 409–435 (2002).

30. Garesse, R. & Vallejo, C. G. Animal mitochondrial biogenesis and function: A regulatory cross-talk between two genomes. *Gene* **263,** 1–16 (2001).

31. Pfanner, N. & Wiedemann, N. Mitochondrial protein import: Two membranes, three translocases. *Current Opinion in Cell Biology* **14,** 400–411 (2002).

32. Alberts, B. *et al. Molecular Biology of the Cell*. *4th Edition, New York* (2002). doi:10.1091/mbc.E14-10-1437

33. Freya, T. G. & Mannellab, C. A. The internal structure of mitochondria. *Trends in Biochemical Sciences* **25,** 319–324 (2000).

34. O'Rourke, B. Mitochondrial Ion Channels. *Annu. Rev. Physiol.* **69,** 19–49 (2007).

35. Lemasters, J. J. & Holmuhamedov, E. Voltage-dependent anion channel (VDAC) as mitochondrial governator - Thinking outside the box. *Biochimica et Biophysica Acta - Molecular Basis of Disease* **1762,** 181–190 (2006).

36. Taanman, J. W. The mitochondrial genome: structure, transcription, translation and replication. *Biochim Biophys Acta* **1410,** 103–23. (1999).

37. Calvo, S. *et al.* Systematic identification of human mitochondrial disease genes through integrative genomics. *Nat Genet* **38,** 576–582 (2006).

38. Becker, T., Vögtle, F.-N., Stojanovski, D. & Meisinger, C. Sorting and assembly of mitochondrial outer membrane proteins. *Biochim. Biophys. Acta* **1777,** 557–63 (2008).

39. Pfanner, N. & Meijer, M. Mitochondrial biogenesis: The Tom and Tim machine. *Curr. Biol.* **7,** R100–R103 (1997).

40. Gilkerson, R. W., Selker, J. M. L. & Capaldi, R. A. The cristal membrane of mitochondria is the principal site of oxidative phosphorylation. *FEBS Lett.* **546,** 355–358 (2003).

41. Vogel, F., Bornhövd, C., Neupert, W. & Reichert, A. S. Dynamic subcompartmentalization of the mitochondrial inner membrane. *J. Cell Biol.* **175,** 237–247 (2006).

42. Herrmann, J. M. & Riemer, J. The intermembrane space of mitochondria. *Antioxid. Redox Signal.* **13,** 1341–1358 (2010).

43. Haruo Sugi, Kobayashi, T., Tsuchiya, T., Chaen, S. & Sugiura, S. Skeletal Muscle - From Myogenesis to Clinical Relations. *Evid. Essent. Role Myosin Head Lever Arm Domain Myosin Subfragment-2 Muscle Contract.* Chapter 6 (2012). doi:10.5772/2961

44. Hatefi, Y. The Mitochondrial Electron Transport and Oxidative Phosphorylation System. *Annu. Rev. Biochem.* **54,** 1015–1069 (1985).

45. Rolfe, D. F. S. & Brown, G. C. Cellular Energy Utilization of Standard Metabolic and Molecular Origin Rate in Mammals. *Physiol. Rev.* **77,** 731–758 (1997).

46. Jastroch, M., Divakaruni, A. S., Mookerjee, S., Treberg, J. R. & Brand, M. D. Mitochondrial proton and electron leaks. *Essays Biochem.* **47,** 53–67 (2010).

47. Brand, M. D. *et al.* The significance and mechanism of mitochondrial proton conductance. *Int. J. Obes. Relat. Metab. Disord.* **23 Suppl 6,** S4–S11 (1999).

48. Abumrad, N. A., El-Maghrabi, M. R., Amri, E. Z., Lopez, E. & Grimaldi, P. A. Cloning of a rat adipocyte membrane protein implicated in binding or transport of long-chain fatty acids that is induced during preadipocyte differentiation.

Homology with human CD36. *J. Biol. Chem.* **268,** 17665–17668 (1993).

49. Glatz, J. F. C., Luiken, J. J. F. P. & Bonen, A. Membrane fatty acid transporters as regulators of lipid metabolism: implications for metabolic disease. *Physiol. Rev.* **90,** 367–417 (2010).

50. Hirsch, D., Stahl, A. & Lodish, H. F. A family of fatty acid transporters conserved from mycobacterium to man. *Proc. Natl. Acad. Sci. U. S. A.* **95,** 8625–9 (1998).

51. Stremmel, W., Strohmeyer, G., Borchard, F., Kochwa, S. & Berk, P. D. Isolation and partial characterization of a fatty acid binding protein in rat liver plasma membranes. *Proc. Natl. Acad. Sci. U. S. A.* **82,** 4–8 (1985).

52. McGarry, J. D. & Brown, N. F. The Mitochondrial Carnitine Palmitoyltransferase System - From Concept to Molecular Analysis. *Eur. J. Biochem.* **244,** 1–14 (1997).

53. Serra, D., Mera, P., Malandrino, M. I., Mir, J. F. & Herrero, L. Mitochondrial Fatty Acid Oxidation in Obesity. *Antioxid. Redox Signal.* **19,** 269–284 (2013).

54. Kiens, B. Skeletal muscle lipid metabolism in exercise and insulin resistance. *Physiol. Rev.* **86,** 205–243 (2006).

55. Schultz, B. E. & Chan, S. I. Structures and proton-pumping strategies of mitochondrial respiratory enzymes. *Annu. Rev. Biophys. Biomol. Struct.* **30,** 23–65 (2001).

56. Mailloux, R. J. Teaching the fundamentals of electron transfer reactions in mitochondria and the production and detection of reactive oxygen species. *Redox Biology* **4,** 381–398 (2015).

57. Efremov, R. G. & Sazanov, L. A. Respiratory complex I: ‘steam engine’ of the cell? *Current Opinion in Structural Biology* **21,** 532–540 (2011).

58. Hirst, J. Mitochondrial complex I. *Annu. Rev. Biochem.* **82,** 551–575 (2013).

59. Berg, J. M., Tymoczko, J. L. & Stryer, L. Biochemistry. *W H Free.* **New York.,** 320–323 (2002).

60. Okuno, D., Iino, R. & Noji, H. Rotation and structure of FoF1-ATP synthase. *Journal of Biochemistry* **149,** 655–664 (2011).

61. Jonckheere, A. I., Smeitink, J. A. M. & Rodenburg, R. J. T. Mitochondrial ATP synthase: Architecture, function and pathology. *Journal of Inherited Metabolic Disease* **35,** 211–225 (2012).

62. Campanella, M., Parker, N., Tan, C. H., Hall, A. M. & Duchen, M. R. IF1: setting the pace of the F1Fo-ATP synthase. *Trends in Biochemical Sciences* **34,** 343–350 (2009).

63. Mitchell, P. Coupling of phosphorylation to electron and hydroegn transfer by a chemi osmotic type of mechanism. *Nature* **191,** 145–191 (1961).

64. Neupert, W. & Herrmann, J. M. Translocation of Proteins into Mitochondria. *Annu. Rev. Biochem.* **76,** 723–749 (2007).

65. Halestrap, A. P. What is the mitochondrial permeability transition pore? *Journal of Molecular and Cellular Cardiology* **46,** 821–831 (2009).

66. Hunter, D. R. & Haworth, R. a. The Ca 2+ - induced membrane transition in mitochondria. *Arch. Biochem. Biophys.* **195,** 468–477 (1979).

67. CROMPTON, M. & COSTI, A. Kinetic evidence for a heart mitochondrial pore activated by Ca2+, inorganic phosphate and oxidative stress: A potential mechanism for mitochondrial dysfunction during cellular Ca2+ overload. *Eur. J. Biochem.* **178,** 489–501 (1988).

68. Griffiths, E. J. & Halestrap, A. P. Mitochondrial non-specific pores remain closed during cardiac ischaemia, but open upon reperfusion. *Biochem. J.* **307 (Pt 1,** 93–8 (1995).

69. CHAPPELL, J. B. & CROFTS, A. R. Calcium Ion Accumulation and Volume Changes of Isolated Liver Mitochondria. Calcium Ion-Induced Swelling. *Biochem. J.* **95,** 378–86 (1965).

70. Turrens, J. F. Mitochondrial formation of reactive oxygen species. *J. Physiol.* **552,** 335–344 (2003).

71. Murphy, M. P. How mitochondria produce reactive oxygen species. *Biochem. J.* **417,** 1–13 (2009).

72. Ni, H. M., Williams, J. A. & Ding, W. X. Mitochondrial dynamics and mitochondrial quality control. *Redox Biology* **4,** 6–13 (2015).

73. Westermann, B. Mitochondrial fusion and fission in cell life and death. *Nat. Rev. Mol. Cell Biol.* **11,** 872–884 (2010).

74. Liesa, M., Palacin, M. & Zorzano, A. Mitochondrial Dynamics in Mammalian Health and Disease. *Physiol. Rev.* **89,** 799–845 (2009).

75. Twig, G., Hyde, B. & Shirihai, O. S. Mitochondrial fusion, fission and autophagy as a quality control axis: The bioenergetic view. *Biochimica et Biophysica Acta - Bioenergetics* **1777,** 1092–1097 (2008).

76. Archer, S. L. Mitochondrial Dynamics - mitochondrial fission and fusion in human diseases. *N. Engl. J. Med.* **369,** 2236–2251 (2013).

77. Youle, R. J. & van der Bliek, A. M. Mitochondrial fission, fusion, and stress. *Science* **337,** 1062–5 (2012).

78. Kiššová, I., Deffieu, M., Manon, S. & Camougrand, N. Uth1p is involved in the autophagic degradation of mitochondria. *J. Biol. Chem.* **279,** 39068–39074 (2004).

79. Koshiba, T. Structural Basis of Mitochondrial Tethering by Mitofusin Complexes. *Science (80-.).* **305,** 858–862 (2004).

80. Bach, D. *et al.* Expression of Mfn2, the Charcot-Marie-Tooth Neuropathy Type 2A Gene, in Human Skeletal Muscle. *Diabetes* **54,** 2685–2693 (2005).

81. Pich, S. *et al.* The Charcot-Marie-Tooth type 2A gene product, Mfn2, up-regulates fuel oxidation through expression of OXPHOS system. *Hum. Mol. Genet.* **14,** 1405–1415 (2005).

82. Frezza, C. *et al.* OPA1 Controls Apoptotic Cristae Remodeling Independently from Mitochondrial Fusion. *Cell* **126,** 177–189 (2006).

83. Meeusen, S. *et al.* Mitochondrial Inner-Membrane Fusion and Crista Maintenance Requires the??Dynamin-Related GTPase Mgm1. *Cell* **127,** 383–395 (2006).

84. Otera, H. *et al.* Mff is an essential factor for mitochondrial recruitment of Drp1 during mitochondrial fission in mammalian cells. *J. Cell Biol.* **191,** 1141–1158 (2010).

85. Elgass, K., Pakay, J., Ryan, M. T. & Palmer, C. S. Recent advances into the understanding of mitochondrial fission. *Biochim. Biophys. Acta* **1833,** 150–61 (2013).

86. Twig, G. *et al.* Fission and selective fusion govern mitochondrial segregation and elimination by autophagy. *EMBO J.* **27,** 433–446 (2008).

87. Gomes, L. C. & Scorrano, L. High levels of Fis1, a pro-fission mitochondrial protein, trigger autophagy. *Biochim. Biophys. Acta - Bioenerg.* **1777,** 860–866

(2008).

88. Lee, Y., Lee, H.-Y., Hanna, R. A. & Gustafsson, A. B. Mitochondrial autophagy by Bnip3 involves Drp1-mediated mitochondrial fission and recruitment of Parkin in cardiac myocytes. *AJP Hear. Circ. Physiol.* **301,** H1924–H1931 (2011).

89. Mizushima, N., Levine, B., Cuervo, A. M. & Klionsky, D. J. Autophagy fights disease through cellular self-digestion. *Nature* **451,** 1069–1075 (2008).

90. Hamacher-Brady, A. & Brady, N. R. Mitophagy programs: Mechanisms and physiological implications of mitochondrial targeting by autophagy. *Cellular and Molecular Life Sciences* **73,** 775–795 (2016).

91. Kubli, D. A. & Gustafsson, Å. B. Mitochondria and mitophagy: The yin and yang of cell death control. *Circulation Research* **111,** 1208–1221 (2012).

92. Suen, D.-F., Narendra, D. P., Tanaka, A., Manfredi, G. & Youle, R. J. Parkin overexpression selects against a deleterious mtDNA mutation in heteroplasmic cybrid cells. *Proc. Natl. Acad. Sci.* **107,** 11835–11840 (2010).

93. Narendra, D., Tanaka, A., Suen, D. F. & Youle, R. J. Parkin is recruited selectively to impaired mitochondria and promotes their autophagy. *J. Cell Biol.* **183,** 795–803 (2008).

94. Vives-Bauza, C. *et al.* PINK1-dependent recruitment of Parkin to mitochondria in mitophagy. *Proc. Natl. Acad. Sci.* **107,** 378–383 (2010).

95. Yang, Y. *et al.* Pink1 regulates mitochondrial dynamics through interaction with the fission/fusion machinery. *Proc. Natl. Acad. Sci.* **105,** 7070–7075 (2008).

96. Geisler, S. *et al.* PINK1/Parkin-mediated mitophagy is dependent on VDAC1 and p62/SQSTM1. *Nat. Cell Biol.* **12,** 119–131 (2010).

97. Gegg, M. E. *et al.* Mitofusin 1 and mitofusin 2 are ubiquitinated in a PINK1/parkin-dependent manner upon induction of mitophagy. *Hum. Mol. Genet.* **19,** 4861–4870 (2010).

98. Poole, A. C., Thomas, R. E., Yu, S., Vincow, E. S. & Pallanck, L. The mitochondrial fusion-promoting factor mitofusin is a substrate of the PINK1/parkin pathway. *PLoS One* **5,** (2010).

99. Wang, X. *et al.* PINK1 and Parkin target miro for phosphorylation and degradation to arrest mitochondrial motility. *Cell* **147,** 893–906 (2011).

100. Seibenhener, M. L. *et al.* Sequestosome 1/p62 Is a Polyubiquitin Chain Binding Protein Involved in Ubiquitin Proteasome Degradation. *Mol. Cell. Biol.* **24,** 8055–8068 (2004).

101. Pankiv, S. *et al.* p62/SQSTM1 binds directly to Atg8/LC3 to facilitate degradation of ubiquitinated protein aggregates by autophagy*[S]. *J. Biol. Chem.* **282,** 24131–24145 (2007).

102. Tooze, S. A. & Yoshimori, T. The origin of the autophagosomal membrane. *Nat. Cell Biol.* **12,** 831–835 (2010).

103. Kim, I., Rodriguez-Enriquez, S. & Lemasters, J. J. Selective degradation of mitochondria by mitophagy. *Archives of Biochemistry and Biophysics* **462,** 245–253 (2007).

104. Zhu, Y. *et al.* Modulation of serines 17 and 24 in the LC3-interacting region of Bnip3 determines pro-survival mitophagy versus apoptosis. *J. Biol. Chem.* **288,** 1099–1113 (2013).

105. Scherz-Shouval, R. & Elazar, Z. ROS, mitochondria and the regulation of

autophagy. *Trends Cell Biol.* **17,** 422–427 (2007).

106. Lemasters, J. J. *et al.* The mitochondrial permeability transition in cell death: a common mechanism in necrosis, apoptosis and autophagy. *Biochim. Biophys. Acta* **1366,** 177–196 (1998).

107. Hill, B. G., Dranka, B. P., Zou, L., Chatham, J. C. & Darley-Usmar, V. M. Importance of the bioenergetic reserve capacity in response to cardiomyocyte stress induced by 4-hydroxynonenal. *Biochem. J.* **424,** 99–107 (2009).

108. Bergamini, E. Autophagy: A cell repair mechanism that retards ageing and age-associated diseases and can be intensified pharmacologically. *Molecular Aspects of Medicine* **27,** 403–410 (2006).

109. Garcia, J. *et al.* Regulation of mitochondrial glutathione redox status and protein glutathionylation by respiratory substrates. *J. Biol. Chem.* **285,** 39646–39654 (2010).

110. Leeuwenburgh, C., Fiebig, R., Chandwaney, R. & Ji, L. L. Aging and exercise training in skeletal muscle: responses of glutathione and antioxidant enzyme systems. *Am J Physiol* **267,** R439-45 (1994).

111. Deneke, S. M. & Fanburg, B. L. Regulation of cellular glutathione. *Am. J. Physiol.* **257,** L163–L173 (1989).

112. Lu, S. C. Glutathione synthesis. *Biochim. Biophys. Acta* **1830,** 3143–53 (2013).

113. Halliwell, B. & Gutteridge, J. M. C. Free radicals in biology and medicine. *J. Free Radic. Biol. Med.* **1,** 331–332 (1985).

114. Mårtensson, J. & Meister, A. Mitochondrial damage in muscle occurs after marked depletion of glutathione and is prevented by giving glutathione monoester. *Proc.*

Natl. Acad. Sci. U. S. A. **86,** 471–5 (1989).

115. Reid, M. B. Plasticity in Skeletal, Cardiac, and Smooth Muscle: Invited Review: Redox modulation of skeletal muscle contraction: what we know and what we don't. *J Appl Physiol* **90,** 724–731 (2001).

116. Zitka, O. *et al.* Redox status expressed as GSH:GSSG ratio as a marker for oxidative stress in paediatric tumour patients. *Oncol. Lett.* **4,** 1247–1253 (2012).

117. Handy, D. E. & Loscalzo, J. Redox Regulation of Mitochondrial Function. *Antioxid. Redox Signal.* **16,** 1323–1367 (2012).

118. Meister, A. Glutathione metabolism and its selective modification. *Journal of Biological Chemistry* **263,** 17205–17208 (1988).

119. Shutt, T., Geoffrion, M., Milne, R. & McBride, H. M. The intracellular redox state is a core determinant of mitochondrial fusion. *EMBO Rep.* **13,** 909–915 (2012).

120. Filomeni, G., Rotilio, G. & Ciriolo, M. R. Cell signalling and the glutathione redox system. *Biochem. Pharmacol.* **64,** 1057–1064 (2002).

121. Pizzorno, J. E. & Katzinger, J. J. Glutathione: Physiological and Clinical Relevance. *J. Restor. Med.* **1,** 24–37 (2012).

122. Schafer, F. Q. & Buettner, G. R. Redox environment of the cell as viewed through the redox state of the glutathione disulfide/glutathione couple. *Free Radical Biology and Medicine* **30,** 1191–1212 (2001).

123. Chai, Y. C., Ashraf, S. S., Rokutan, K., Johnston, R. B. & Thomas, J. A. S-thiolation of individual human neutrophil proteins including actin by stimulation of the respiratory burst: evidence against a role for glutathione disulfide. *Arch. Biochem. Biophys.* **310,** 273–281 (1994).

124. Noctor, G., Queval, G., Mhamdi, A., Chaouch, S. & Foyer, C. H. Glutathione. *Arabidopsis Book* **9,** e0142 (2011).

125. Marí, M., Morales, A., Colell, A., García-Ruiz, C. & Fernández-Checa, J. C. Mitochondrial Glutathione, a Key Survival Antioxidant. *Antioxid. Redox Signal.* **11,** 2685–2700 (2009).

126. Griffith, O. W. & Meister, A. Origin and turnover of mitochondrial glutathione. *Proc. Natl. Acad. Sci.* **82,** 4668–4672 (1985).

127. Marí, M. *et al.* Mitochondrial glutathione: Features, regulation and role in disease. *Biochimica et Biophysica Acta - General Subjects* **1830,** 3317–3328 (2013).

128. Meister, A. Mitochondrial changes associated with glutathione deficiency. *BBA - Mol. Basis Dis.* **1271,** 35–42 (1995).

129. Mårtensson, J. *et al.* Inhibition of glutathione synthesis in the newborn rat: a model for endogenously produced oxidative stress. *Proc. Natl. Acad. Sci. U. S. A.* **88,** 9360–4 (1991).

130. Griffith, O. W. & Mulcahy, R. T. *The enzymes of glutathione synthesis: gamma-glutamylcysteine synthetase. Advances in enzymology and related areas of molecular biology* **73,** (1999).

131. Aquilano, K., Baldelli, S. & Ciriolo, M. R. Glutathione: New roles in redox signalling for an old antioxidant. *Frontiers in Pharmacology* **5 AUG,** (2014).

132. Smith, J. E., Moore, K. & Board, P. G. Regulation of gamma-glutamylcysteine utilization in erythrocytes. *Enzyme* **25,** 236–240 (1980).

133. Meister, A. & Anderson, M. E. Glutathione. *Annu. Rev. Biochem.* **52,** 711–760 (1983).

134. Chen, Y., Shertzer, H. G., Schneider, S. N., Nebert, D. W. & Dalton, T. P. Glutamate cysteine ligase catalysis: Dependence on ATP and modifier subunit for regulation of tissue glutathione levels. *J. Biol. Chem.* **280,** 33766–33774 (2005).

135. Anderson, M. E. & Meister, A. Transport and direct utilization of gamma-glutamylcyst(e)ine for glutathione synthesis. *Proc. Natl. Acad. Sci. U. S. A.* **80,** 707–11 (1983).

136. Richman, P. G. & Meister, A. Regulation of ?? glutamyl cysteine synthetase by nonallosteric feedback inhibition by glutathione. *J. Biol. Chem.* **250,** 1422–1426 (1975).

137. Bridges, R. J., Natale, N. R. & Patel, S. A. System x c - cystine/glutamate antiporter: An update on molecular pharmacology and roles within the CNS. *British Journal of Pharmacology* **165,** 20–34 (2012).

138. Griffith, O. W. Biologic and pharmacologic regulation of mammalian glutathione synthesis. in *Free Radical Biology and Medicine* **27,** 922–935 (1999).

139. Lushchak, V. I. Glutathione Homeostasis and Functions: Potential Targets for Medical Interventions. *J. Amino Acids* **2012,** 1–26 (2012).

140. Go, Y. M. & Jones, D. P. Redox compartmentalization in eukaryotic cells. *Biochimica et Biophysica Acta - General Subjects* **1780,** 1273–1290 (2008).

141. Ciriolo, M. R., Aquilano, K., De Martino, A., Carrì, M. T. & Rotilio, G. Differential role of superoxide and glutathione in S-nitrosoglutathione-mediated apoptosis: A rationale for mild forms of familial amyotrophic lateral sclerosis associated with less active Cu,Zn superoxide dismutase mutants. *J. Neurochem.* **77,** 1433–1443 (2001).

142. Aquilano, K., Vigilanza, P., Rotilio, G. & Ciriolo, M. R. Mitochondrial damage due to SOD1 deficiency in SH-SY5Y neuroblastoma cells: a rationale for the redundancy of SOD1. *FASEB J.* **20,** 1683–1685 (2006).

143. Legault, J. *et al.* Mitochondrial GPx1 Decreases Induced but Not Basal Oxidative Damage to mtDNA in T47D Cells. *Biochem. Biophys. Res. Commun.* **272,** 416–422 (2000).

144. Comporti, M. Glutathione depleting agents and lipid peroxidation. *Chem. Phys. Lipids* **45,** 143–169 (1987).

145. Pompella, A., Visvikis, A., Paolicchi, A., De Tata, V. & Casini, A. F. The changing faces of glutathione, a cellular protagonist. in *Biochemical Pharmacology* **66,** 1499–1503 (2003).

146. Holmgren, A. Hydrogen donor system for Escherichia coli ribonucleoside-diphosphate reductase dependent upon glutathione. *Proc. Natl. Acad. Sci. U. S. A.* **73,** 2275–2279 (1976).

147. Morell, S., Follmann, H. & H??berlein, I. Identification and localization of the first glutaredoxin in leaves of a higher plant. *FEBS Lett.* **369,** 149–152 (1995).

148. Cho, Y. W., Kim, J. C., Jin, C. D., Han, T. J. & Lim, C. J. Thioltransferase from Arabidopsis thaliana seed: purification to homogeneity and characterization. *Mol Cells* **8,** 550–5. (1998).

149. Ahn, B. Y. & Moss, B. Glutaredoxin homolog encoded by vaccinia virus is a virion-associated enzyme with thioltransferase and dehydroascorbate reductase activities. *Proc. Natl. Acad. Sci. U. S. A.* **89,** 7060–7064 (1992).

150. Eklund, H. *et al.* Structure of oxidized bacteriophage T4 glutaredoxin

(thioredoxin). Refinement of native and mutant proteins. *J. Mol. Biol.* **228,** 596–618 (1992).

151. Hopper, S., Johnson, R. S., Vath, J. E. & Biemann, K. Glutaredoxin from rabbit bone marrow. Purification, characterization, and amino acid sequence determined by tandem mass spectrometry. *J Biol Chem* **264,** 20438–20447 (1989).

152. Padilla, C. A., Mart??nez???Galisteo, E., B??rcena, J. A., Spyrou, G. & Holmgren, A. Purification from Placenta, Amino Acid Sequence, Structure Comparisons and cDNA Cloning of Human Glutaredoxin. *Eur. J. Biochem.* **227,** 27–34 (1995).

153. Kalinina, E. V, Chernov, N. N. & Saprin, a N. Involvement of thio-, peroxi-, and glutaredoxins in cellular redox-dependent processes. *Biochemistry. (Mosc).* **73,** 1493–1510 (2008).

154. Hanschmann, E.-M., Godoy, J. R., Berndt, C., Hudemann, C. & Lillig, C. H. Thioredoxins, Glutaredoxins, and Peroxiredoxins—Molecular Mechanisms and Health Significance: from Cofactors to Antioxidants to Redox Signaling. *Antioxid. Redox Signal.* **19,** 1539–1605 (2013).

155. H????G, J. ???O, J??RNVALL, H., HOLMGREN, A., CARLQUIST, M. & PERSSON, M. The primary structure of Escherichia coli glutaredoxin: Distant homology with thioredoxins in a superfamily of small proteins with a redox???active cystine disulfide/cysteine dithiol. *Eur. J. Biochem.* **136,** 223–232 (1983).

156. Rozell, B., Barcena, J. A., Martinez-Galisteo, E., Padilla, C. A. & Holmgren, A. Immunochemical characterization and tissue distribution of glutaredoxin (thioltransferase) from calf. *Eur J Cell Biol* **62,** 314–323 (1993).

157. Lundberg, M., Fernandes, A. P., Kumar, S. & Holmgren, A. Cellular and plasma levels of human glutaredoxin 1 and 2 detected by sensitive ELISA systems. *Biochem. Biophys. Res. Commun.* **319,** 801–809 (2004).

158. Pai, H. V., Starke, D. W., Lesnefsky, E. J., Hoppel, C. L. & Mieyal, J. J. What is the Functional Significance of the Unique Location of Glutaredoxin 1 (GRx1) in the Intermembrane Space of Mitochondria? *Antioxid. Redox Signal.* **9,** 2027–2034 (2007).

159. Aesif, S. W. *et al.* Ablation of glutaredoxin-1 attenuates lipopolysaccharide-induced lung inflammation and alveolar macrophage activation. *Am. J. Respir. Cell Mol. Biol.* **44,** 491–499 (2011).

160. Bachschmid, M. M. *et al.* Attenuated cardiovascular hypertrophy and oxidant generation in response to angiotensin II infusion in glutaredoxin-1 knockout mice. *Free Radic. Biol. Med.* **49,** 1221–1229 (2010).

161. Lundberg, M. *et al.* Cloning and Expression of a Novel Human Glutaredoxin (Grx2) with Mitochondrial and Nuclear Isoforms. *J. Biol. Chem.* **276,** 26269–26275 (2001).

162. Jurado, J., Prieto-Álamo, M. J., Madrid-Rísquez, J. & Pueyo, C. Absolute Gene Expression Patterns of Thioredoxin and Glutaredoxin Redox Systems in Mouse. *J. Biol. Chem.* **278,** 45546–45554 (2003).

163. Fernando, M. R., Lechner, J. M., Löfgren, S., Gladyshev, V. N. & Lou, M. F. Mitochondrial thioltransferase (glutaredoxin 2) has GSH-dependent and thioredoxin reductase-dependent peroxidase activities in vitro and in lens epithelial cells. *FASEB J.* **20,** 2645–2647 (2006).

164. Johansson, C., Lillig, C. H. & Holmgren, A. Human Mitochondrial Glutaredoxin Reduces S-Glutathionylated Proteins with High Affinity Accepting Electrons from Either Glutathione or Thioredoxin Reductase. *J. Biol. Chem.* **279,** 7537–7543 (2004).

165. Beer, S. M. *et al.* Glutaredoxin 2 catalyzes the reversible oxidation and glutathionylation of mitochondrial membrane thiol proteins: Implications for mitochondrial redox regulation and antioxidant defense. *J. Biol. Chem.* **279,** 47939–47951 (2004).

166. Hurd, T. R. *et al.* Complex I within oxidatively stressed bovine heart mitochondria is glutathionylated on Cys-531 and Cys-704 of the 75-kDa subunit: Potential role of Cys residues in decreasing oxidative damage. *J. Biol. Chem.* **283,** 24801–24815 (2008).

167. Lillig, C. H., Lönn, M. E., Enoksson, M., Fernandes, A. P. & Holmgren, A. Short interfering RNA-mediated silencing of glutaredoxin 2 increases the sensitivity of HeLa cells toward doxorubicin and phenylarsine oxide. *Proc. Natl. Acad. Sci. U. S. A.* **101,** 13227–32 (2004).

168. Mailloux, R. J. *et al.* Glutaredoxin-2 is required to control proton leak through uncoupling protein-3. *J. Biol. Chem.* **288,** 8365–8379 (2013).

169. Lillig, C. H., Berndt, C. & Holmgren, A. Glutaredoxin systems. *Biochimica et Biophysica Acta - General Subjects* **1780,** 1304–1317 (2008).

170. Cha, H. *et al.* PICOT is a critical regulator of cardiac hypertrophy and cardiomyocyte contractility. *J. Mol. Cell. Cardiol.* **45,** 796–803 (2008).

171. Wingert, R. A. *et al.* Deficiency of glutaredoxin 5 reveals Fe–S clusters are

required for vertebrate haem synthesis. *Nature* **436,** 1035–1039 (2005).

172. Rodriguez-Manzaneque, M. T. Grx5 Is a Mitochondrial Glutaredoxin Required for the Activity of Iron/Sulfur Enzymes. *Mol. Biol. Cell* **13,** 1109–1121 (2002).

173. Linares, G. R., Xing, W., Govoni, K. E., Chen, S. T. & Mohan, S. Glutaredoxin 5 regulates osteoblast apoptosis by protecting against oxidative stress. *Bone* **44,** 795–804 (2009).

174. Molina-Navarro, M. M., Casas, C., Piedrafita, L., Bellí, G. & Herrero, E. Prokaryotic and eukaryotic monothiol glutaredoxins are able to perform the functions of Grx5 in the biogenesis of Fe/S clusters in yeast mitochondria. *FEBS Lett.* **580,** 2273–2280 (2006).

175. Lönn, M. E. *et al.* Expression Pattern of Human Glutaredoxin 2 Isoforms: Identification and Characterization of Two Testis/Cancer Cell-Specific Isoforms. *Antioxid. Redox Signal.* **10,** 547–558 (2008).

176. Dalle-Donne, I., Rossi, R., Colombo, G., Giustarini, D. & Milzani, A. Protein S-glutathionylation: a regulatory device from bacteria to humans. *Trends in Biochemical Sciences* **34,** 85–96 (2009).

177. Ribas, V., García-Ruiz, C. & Fernández-Checa, J. C. Glutathione and mitochondria. *Frontiers in Pharmacology* **5 JUL,** (2014).

178. Silva, G. M. *et al.* Role of glutaredoxin 2 and cytosolic thioredoxins in cysteinyl-based redox modification of the 20S proteasome. *FEBS J.* **275,** 2942–2955 (2008).

179. Gladyshev, V. N. *et al.* Identification and Characterization of a New Mammalian Glutaredoxin (Thioltransferase), Grx2. *J. Biol. Chem.* **276,** 30374–30380 (2001).

180. Jung, C.-H. & Thomas, J. A. S-Glutathiolated Hepatocyte Proteins and Insulin

Disulfides as Substrates for Reduction by Glutaredoxin, Thioredoxin, Protein Disulfide Isomerase, and Glutathione. *Arch. Biochem. Biophys.* **335,** 61–72 (1996).

181. Clavreul, N. S-glutathiolation by peroxynitrite of p21ras at cysteine-118 mediates its direct activation and downstream signaling in endothelial cells. *FASEB J.* (2006). doi:10.1096/fj.05-4875fje

182. Qanungo, S., Starke, D. W., Pai, H. V., Mieyal, J. J. & Nieminen, A. L. Glutathione supplementation potentiates hypoxic apoptosis by S-glutathionylation of p65-NF??B. *J. Biol. Chem.* **282,** 18427–18436 (2007).

183. Gilbert, H. F. Redox control of enzyme activities by thiol/disulfide exchange. *Methods Enzymol.* **107,** 330–351 (1984).

184. Di Simplicio, P. *et al.* Role of protein -SH groups in redox homeostasis--the erythrocyte as a model system. *Arch. Biochem. Biophys.* **355,** 145–152 (1998).

185. Gravina, S. A. & Mieyal, J. J. Thioltransferase is a specific glutathionyl mixed disulfide oxidoreductase. *Biochemistry* **32,** 3368–3376 (1993).

186. Ruoppolo, M., Lundström-Ljung, J., Talamo, F., Pucci, P. & Marino, G. Effect of glutaredoxin and protein disulfide isomerase on the glutathione-dependent folding of ribonuclease A. *Biochemistry* **36,** 12259–12267 (1997).

187. Kang, P. T. *et al.* Protein thiyl radical mediates S-glutathionylation of complex i. *Free Radic. Biol. Med.* **53,** 962–973 (2012).

188. Taylor, E. R. *et al.* Reversible glutathionylation of complex I increases mitochondrial superoxide formation. *J. Biol. Chem.* **278,** 19603–19610 (2003).

189. Hurd, T. R. *et al.* Glutathionylation of Mitochondrial Proteins. *Antioxid. Redox Signal.* **7,** 999–1010 (2005).

190. Murphy, M. P. Mitochondrial Thiols in Antioxidant Protection and Redox Signaling: Distinct Roles for Glutathionylation and Other Thiol Modifications. *Antioxid. Redox Signal.* **16,** 476–495 (2012).

191. Shelton, M. D., Chock, P. B. & Mieyal, J. J. Glutaredoxin: role in reversible protein s-glutathionylation and regulation of redox signal transduction and protein translocation. *Antioxid. Redox Signal.* **7,** 348–366 (2005).

192. Pesta, D. & Gnaiger, E. High-resolution respirometry: OXPHOS protocols for human cells and permeabilized fibers from small biopsies of human muscle. *Methods Mol. Biol.* **810,** 25–58 (2012).

193. Pasut, A., Oleynik, P. & Rudnicki, M. A. Isolation of muscle stem cells by fluorescence activated cell sorting cytometry. *Methods Mol. Biol.* **798,** 53–64 (2012).

194. Zong, H. *et al.* AMP kinase is required for mitochondrial biogenesis in skeletal muscle in response to chronic energy deprivation. *Proc. Natl. Acad. Sci.* **99,** 15983–15987 (2002).

195. Guo, W., Jiang, L., Bhasin, S., Khan, S. M. & Swerdlow, R. H. DNA extraction procedures meaningfully influence qPCR-based mtDNA copy number determination. *Mitochondrion* **9,** 261–265 (2009).

196. Langan, T. J. & Chou, R. C. Synchronization of mammalian cell cultures by serum deprivation. *Methods Mol. Biol.* **761,** 75–83 (2011).

197. Mailloux, R. J. *et al.* Glutaredoxin-2 Is required to control oxidative phosphorylation in cardiac muscle by mediating deglutathionylation reactions. *J. Biol. Chem.* **289,** 14812–14828 (2014).

198. Huang, J., Lam, G. Y. & Brumell, J. H. Autophagy Signaling Through Reactive Oxygen Species. *Antioxid. Redox Signal.* **14,** 2215–2231 (2011).

199. Martina, J. A., Chen, Y., Gucek, M. & Puertollano, R. MTORC1 functions as a transcriptional regulator of autophagy by preventing nuclear transport of TFEB. *Autophagy* **8,** 903–914 (2012).

200. Kim, J., Kundu, M., Viollet, B. & Guan, K.-L. AMPK and mTOR regulate autophagy through direct phosphorylation of Ulk1. *Nat. Cell Biol.* **13,** 132–141 (2011).

201. Morino, K. *et al.* Reduced mitochondrial density and increased IRS-1 serine phosphorylation in muscle of insulin-resistant offspring of type 2 diabetic parents. *J. Clin. Invest.* **115,** 3587–3593 (2005).

202. Larsen, S. *et al.* Biomarkers of mitochondrial content in skeletal muscle of healthy young human subjects. *J. Physiol.* **590,** 3349–3360 (2012).

203. Detmer, S. A. & Chan, D. C. Functions and dysfunctions of mitochondrial dynamics. *Nat. Rev. Mol. Cell Biol.* **8,** 870–879 (2007).

204. Suen, D. F., Norris, K. L. & Youle, R. J. Mitochondrial dynamics and apoptosis. *Genes and Development* **22,** 1577–1590 (2008).

205. Hoppins, S., Lackner, L. & Nunnari, J. The Machines that Divide and Fuse Mitochondria. *Annu. Rev. Biochem.* **76,** 751–780 (2007).

206. Chen, H. *et al.* Mitochondrial fusion is required for mtdna stability in skeletal muscle and tolerance of mtDNA mutations. *Cell* **141,** 280–289 (2010).

207. Cogliati, S., Enriquez, J. A. & Scorrano, L. Mitochondrial Cristae: Where Beauty Meets Functionality. *Trends in Biochemical Sciences* **41,** 261–273 (2016).

208. Zick, M., Rabl, R. & Reichert, A. S. Cristae formation-linking ultrastructure and function of mitochondria. *Biochimica et Biophysica Acta - Molecular Cell Research* **1793,** 5–19 (2009).

209. Hackenbrock, C. R. Ultrastructural bases for metabolically linked mechanical activity in mitochondria. I. Reversible ultrastructural changes with change in metabolic steady state in isolated liver mitochondria. *J. Cell Biol.* **30,** 269–297 (1966).

210. Scorrano, L. *et al.* A distinct pathway remodels mitochondrial cristae and mobilizes cytochrome c during apoptosis. *Dev. Cell* **2,** 55–67 (2002).

211. Natale, G. *et al.* Compartment-dependent mitochondrial alterations in experimental ALS, the effects of mitophagy and mitochondriogenesis. *Front. Cell. Neurosci.* **9,** (2015).

212. Martinou, J. C. & Green, D. R. Breaking the mitochondrial barrier. *Nat. Rev. Mol. Cell Biol.* **2,** 63–67 (2001).

213. Kroemer, G., Galluzzi, L. & Brenner, C. Mitochondrial membrane permeabilization in cell death. *Physiol. Rev.* **87,** 99–163 (2007).

214. Montero, J. *et al.* Cholesterol and peroxidized cardiolipin in mitochondrial membrane properties, permeabilization and cell death. *Biochimica et Biophysica Acta - Bioenergetics* **1797,** 1217–1224 (2010).

215. Hansen, J. M., Go, Y.-M. & Jones, D. P. NUCLEAR AND MITOCHONDRIAL COMPARTMENTATION OF OXIDATIVE STRESS AND REDOX SIGNALING. *Annu. Rev. Pharmacol. Toxicol.* **46,** 215–234 (2006).

216. Kemp, M., Go, Y.-M. & Jones, D. P. Nonequilibrium thermodynamics of

thiol/disulfide redox systems: a perspective on redox systems biology. *Free Radic. Biol. Med.* **44,** 921–37 (2008).

217. Won, J. S. & Singh, I. Sphingolipid signaling and redox regulation. *Free Radical Biology and Medicine* **40,** 1875–1888 (2006).

218. Sykes, M. C., Mowbray, A. L. & Jo, H. Reversible glutathiolation of caspase-3 by glutaredoxin as a novel redox signaling mechanism in tumor necrosis factor-α-induced cell death. *Circulation Research* **100,** 152–154 (2007).

219. Franco, R. & Cidlowski, J. a. Apoptosis and glutathione: beyond an antioxidant. *Cell Death Differ.* **16,** 1303–1314 (2009).

220. Circu, M. L. & Yee Aw, T. Glutathione and apoptosis. *Free Radic. Res.* **42,** 689–706 (2008).

221. Enoksson, M. *et al.* Overexpression of glutaredoxin 2 attenuates apoptosis by preventing cytochrome c release. *Biochem. Biophys. Res. Commun.* **327,** 774–779 (2005).

222. Armstrong, J. S. & Jones, D. P. Glutathione depletion enforces the mitochondrial permeability transition and causes cell death in Bcl-2 overexpressing HL60 cells. *FASEB J.* **16,** 1263–1265 (2002).

223. Underwood, B. R. *et al.* Antioxidants can inhibit basal autophagy and enhance neurodegeneration in models of polyglutamine disease. *Hum. Mol. Genet.* **19,** 3413–3429 (2010).

224. Lin, T. C. *et al.* Autophagy: Resetting glutamine-dependent metabolism and oxygen consumption. *Autophagy* **8,** 1477–1493 (2012).

225. Meredith, M. J. & Reed, D. J. Status of the mitochondrial pool of glutathione in

the isolated hepatocyte. *J. Biol. Chem.* **257,** 3747–3753 (1982).

226. Olafsdottir, K. & Reed, D. J. Retention of oxidized glutathione by isolated rat liver mitochondria during hydroperoxide treatment. *BBA - Gen. Subj.* **964,** 377–382 (1988).

227. Kroemer, G. Mitochondrial control of apoptosis: an overview. *Biochem. Soc. Symp.* **66,** 1–15 (1999).

228. Lovy, A., Molina, A. J. A., Cerqueira, F. M., Trudeau, K. & Shirihai, O. S. A Faster, High Resolution, mtPA-GFP-based Mitochondrial Fusion Assay Acquiring Kinetic Data of Multiple Cells in Parallel Using Confocal Microscopy. *J. Vis. Exp.* (2012). doi:10.3791/3991

229. Franco, R., Schoneveld, O. J., Pappa, A. & Panayiotidis, M. I. The central role of glutathione in the pathophysiology of human diseases. *Arch. Physiol. Biochem.* **113,** 234–58 (2007).

230. Rolo, A. P. & Palmeira, C. M. Diabetes and mitochondrial function: Role of hyperglycemia and oxidative stress. *Toxicology and Applied Pharmacology* **212,** 167–178 (2006).

231. Obrosova, I. G., Fathallah, L. & Greene, D. a. Early changes in lipid peroxidation and antioxidative defense in diabetic rat retina: effect of DL-alpha-lipoic acid. *Eur. J. Pharmacol.* **398,** 139–146 (2000).

232. Sharma, A., Kharb, S., Chugh, S. N., Kakkar, R. & Singh, G. P. Evaluation of oxidative stress before and after control of glycemia and after vitamin E supplementation in diabetic patients. *Metabolism.* **49,** 160–162 (2000).

233. Sampathkumar, R. *et al.* Increased glutathionylated hemoglobin (HbSSG) in type 2

diabetes subjects with microangiopathy. *Clin. Biochem.* **38,** 892–899 (2005).